

# Principal stratification with recurrent events truncated by a terminal event: A nested Bayesian nonparametric approach

Yuki Ohnishi

Department of Biostatistics, Yale School of Public Health,

Michael O. Harhay

Department of Biostatistics, Epidemiology and Informatics,

University of Pennsylvania,

and

Fan Li

Department of Biostatistics, Yale School of Public Health

December 1, 2025

## Abstract

Recurrent events often serve as key endpoints in clinical studies but may be prematurely truncated by terminal events such as death, creating selection bias and complicating causal inference. To address this challenge, we propose novel causal estimands within the principal stratification framework, introducing a refined always-survivor stratum that defines survival until the final recurrent event rather than a fixed time point, yielding more stable causal contrasts. We develop a flexible Bayesian nonparametric prior—the enriched dependent Dirichlet process—specifically designed for joint modeling of recurrent and terminal events, addressing a limitation where standard Dirichlet process priors create random partitions dominated by recurrent events, yielding poor predictive performance for terminal events. Our nested structure separates within-arm and cross-arm dependence through a dual-frailty framework, enabling transparent sensitivity analysis for non-identifiable parameters. Simulations are carried out to show that our method has superior performance compared to existing methods. We also illustrate the proposed Bayesian methods to infer the causal effect of intensive blood pressure control on recurrent cardiovascular events in a cardiovascular clinical trial.

*Keywords: Causal inference; Bayesian nonparametric methods; Principal stratification; Semi-competing risks; Enriched dependent Dirichlet process*

# 1 Introduction

Recurrent events are commonly observed in clinical trials and observational studies. Examples include hospitalizations or exacerbations of illness, and recurrent endpoints can provide valuable insights into the disease burden. Thus, the ability to draw valid causal inference about treatment effects on recurrent events can facilitate informed decision-making. Nonetheless, analyzing recurrent events becomes complex in the presence of a terminal survival event, since the death can introduce selection bias, because patients who die under one treatment condition may systematically differ in their baseline risk profiles from those who remain alive. In such cases, standard regression analyses may yield inaccurate conclusions about the treatment efficacy, since the estimated effects may primarily reflect differences in susceptible risk profiles rather than genuine causal effects on the recurrent process.

Principal stratification (Frangakis and Rubin, 2002) is a general framework for causal inference that involves post-treatment intermediate variables and has gained prominence in addressing complexities caused by truncation due to death. Within this framework, subpopulations—known as principal strata—are defined by intermediate potential outcomes under each treatment condition, enabling researchers to define unambiguous causal effects within these subgroups. For example, the always-survivor subpopulation, consisting of patients who would survive until the non-terminal event occurs regardless of treatment assignment, was first introduced by Robins (1986) and formally established by Zhang and Rubin (2003). The associated identifiability assumptions have been previously studied when a non-mortality outcome is truncated by death (e.g., Zhang and Rubin, 2003).

Leveraging the principal stratification framework, a flourishing line of research has focused on evaluating the causal effect of treatment on a non-recurrent time-to-event outcome subject to semi-competing risks by death (Comment et al., 2019; Xu et al., 2022; Nevo and

Gorfine, 2022). By contrast, much fewer attention was devoted to identifying causal effects on recurrent events subject to semi-competing risks by death, in which the recurrent event process may be informatively truncated by death. An exception is Lyu et al. (2023), who proposed a causal estimand for the average number of recurrent events among always-survivors and developed a Bayesian parametric joint modeling approach to simultaneously represent the recurrent event and death processes. In their formulation, a single time index  $t$  was used to define both the number of recurrent events and the always-survivor stratum. However, adopting a single time point  $t$  to define causal estimands for recurrent event analysis with a terminal event can be less ideal because it considers the always-survivor population only at that specific time. This perspective makes the subpopulation under study vary by  $t$ , overlooking how treatment effects may accumulate or change over time for a fixed subpopulation and impeding comparisons of estimands across different time points. Additionally, this traditional definition of always-survivors may unnecessarily exclude units from the always-survivor stratum in the context of recurrent events. Finally, principal stratification typically requires careful parametric model specification that encompasses stringent regression assumptions and prior distributions. Therefore, the parametric modeling approach (e.g., Comment et al., 2019; Lyu et al., 2023) could be susceptible to model misspecification bias, especially under potentially complex data generating processes.

To address these challenges, we develop a nested Bayesian nonparametric approach for causal inference with recurrent events in the presence of a terminal event. Our contributions to the literature are several-folded. First, we propose new causal estimands tailored for recurrent event analyses subject to semi-competing risks by death. We explain the limitations of the existing definition of always-survivors for causal recurrent event analysis and introduce refined estimands that are more robust to the choice of time index and

better capture treatment effects over time. We then consider a sensitivity approach to derive the identification results under a principal stratification framework. In addition to identification, our second contribution is to develop a flexible Bayesian nonparametric (BNP) approach for inference. BNP approaches have been increasingly used for recurrent event analysis to mitigate biases arising from model misspecification, a concern in many existing parametric approaches. In both causal and non-causal contexts, previous efforts have employed Dirichlet process (DP) priors to jointly model the recurrent event and terminal event processes (e.g., Paulon et al., 2020; Tian et al., 2024). We discuss in detail a potential pitfall wherein a commonly used DP prior induces a random partition primarily determined by the recurrent events, underestimating the effect of the terminal event. As an improvement, we introduce a nested structure in the DP prior and incorporate dependence on covariates to relax the stringent exchangeability assumption. We refer to our new prior as the enriched dependent Dirichlet process (EDDP) prior, and we develop a fully tractable, efficient Gibbs sampling algorithm for implementation. Third, we introduce a joint-frailty framework for causal inference that cleanly separates within-arm (identifiable) and cross-arm (non-identifiable) dependence. This is in contrast to existing frailty-based causal methods (e.g., Comment et al., 2019; Lyu et al., 2023), which assume a single common frailty, thereby conflating two distinct layers of dependence: (i) the within-arm dependence between recurrent and survival events, and (ii) the cross-arm dependence between potential outcomes under treatment and control. In our approach, each individual instead carries two latent frailties, one per each treatment arm, whose marginal distributions are estimated nonparametrically, while their unidentifiable correlation is treated as an interpretable sensitivity parameter. By varying the sensitivity parameter within a Bayesian g-computation scheme, we transparently track how causal conclusions might

shift under different cross-world dependence structures. Finally, through simulations, we demonstrate that our methods outperform existing approaches in terms of accuracy and robustness. Our proposed methodology is illustrated by re-analyzing recurrent event data from a randomized clinical trial.

## 1.1 A motivating example

The Systolic Blood Pressure Intervention Trial (SPRINT) is a randomized clinical trial that tested whether targeting a systolic blood pressure (SBP) below 120 mm Hg, rather than the conventional goal of below 140 mm Hg, would reduce cardiovascular morbidity and mortality in adults at elevated cardiovascular risk (SPRINT Research Group et al., 2015). A total of 9361 participants aged 50 years or older were randomly assigned in a 1:1 ratio to an intensive-treatment strategy—monthly medication adjustments to achieve SBP < 120 mm Hg—or a standard-treatment strategy involving quarterly visits to maintain SBP 135–139 mm Hg under a prespecified antihypertensive formulary.

In SPRINT, every occurrence of the cardiovascular events that define the primary composite outcome is date-stamped. These events are myocardial infarction, non-MI acute coronary syndrome, stroke, heart-failure decompensation requiring intravenous therapy in a hospital or emergency setting, and cardiovascular death attributed to coronary, cerebrovascular, or other vascular causes. Survival endpoints further include the composite cardiovascular outcome and all-cause mortality. For causal analysis of the SPRINT trial, we use both the counts and timing of non-fatal cardiovascular events to measure the burden of adverse encounters under each SBP target regimen. By tracking each participant’s sequence of events alongside the terminal event, we are interested in the causal comparison between the intensive and standard treatment arms on the total number of events as well

as the rate of event occurrence. To mitigate bias introduced by death, we concentrate on the treatment effect within subpopulations whose recurrent events are not truncated by the terminal event.

## 2 Notation, Setup, and Estimands

We consider a study involving  $n$  units, each assigned to one of two treatment arms at the beginning of the study:  $Z_i = 1$  for the treatment group and  $Z_i = 0$  for the control group. For unit  $i$ , let  $D_i^z$  denote the potential time to death under treatment  $z \in \{0, 1\}$ . The observed survival time is denoted by  $\mathcal{T}_i = \min(D_i^{Z_i}, C_i^{Z_i})$ , where  $C_i^{Z_i}$  denotes the potential censoring time due to loss to follow-up for any reason other than the survival event under the assigned treatment. The event indicators  $\delta_i^D = \mathbb{1}\{\mathcal{T}_i = D_i^{Z_i}\}$  and  $\delta_i^C = \mathbb{1}\{\mathcal{T}_i = C_i^{Z_i}\}$  represent that the observed survival time corresponds to death ( $\delta_i^D = 1$ ) or loss to follow up censoring ( $\delta_i^C = 1$ ), respectively. We assume that the potential cumulative number of recurrent events for subject  $i$  under treatment  $z$ ,  $N_i^z(\cdot)$ , follows a point process. The potential point process  $N_i^z(t)$  is well-defined only for  $0 \leq t < D_i^z$  and undefined for  $t \geq D_i^z$  due to truncation (that is, we use  $N_i^z(t) = *$  for the undefined case). Let  $N_i = N_i^{Z_i}(\mathcal{T}_i)$  denote the observed number of recurrent events until the last follow-up. Let  $T_{ij}^z$  represent the time of the  $j$ -th recurrent event for subject  $i$  under treatment  $z$  for any  $j \in \mathbb{N}$ . Since the recurrent event is truncated for those who experience the terminal event, we define  $T_{ij}^z = *$  for all  $j$  with  $T_{ij}^z > D_i^z$ . As a special case, we write  $T_{i0}^z = 0$ . The observed event times are  $T_{ij} = T_{ij}^{Z_i}$ , which are observed only for  $j$  with  $T_{ij} \leq \mathcal{T}_i$ . The observed event times are  $\{T_{ij}\}_{j=1}^{N_i}$ , and the gap time between two successive events is defined as  $W_{i1}^z = T_{i1}^z$  and  $W_{ij}^z = T_{ij}^z - T_{i(j-1)}^z$ , for  $j \geq 2$ . For the observed data, the gap times are  $W_{ij} = T_{ij} - T_{i(j-1)}$ . Finally, let  $\mathbf{X}_i \in \mathcal{X}$  denote a vector of baseline covariates for unit  $i$ . The observed data for

each unit then consist of the tuple  $O_i = \{\mathcal{T}_i, \delta_i^D, \delta_i^C, N_i, \{T_{ij}\}_{j=1}^{N_i}, Z_i, \mathbf{X}_i\}$ . We consider the following identification assumptions.

**Assumption 1** (Consistency).  $N_i(t) = Z_i N_i^1(t) + (1 - Z_i) N_i^0(t)$ .

**Assumption 2** (Treatment ignorability).  $Z_i \perp \{N_i^0(t), D_i^0, N_i^1(t), D_i^1\} \mid \mathbf{X}_i$ .

**Assumption 3** (Covariate-dependent censoring).  $\{C_i^0, C_i^1\} \perp \{N_i^0(t), D_i^0, N_i^1(t), D_i^1\} \mid \mathbf{X}_i$ .

Assumptions 1 and 2 are standard in randomized trials and observational studies. The first condition assumes away interference and the second condition assumes away any unmeasured confounders, and is guaranteed to hold under randomization. Assumption 3 states that potential censoring times are conditionally independent of the potential event outcomes, and is a common assumption in causal survival analysis. Although empirically unverifiable due to the cross-world counterfactuals, this assumption is reasonable in SPRINT because the majority of right-censored events were due to pre-specified end of follow-up.

## 2.1 Principal stratification in continuous time

Principal stratification (Frangakis and Rubin, 2002) is a general framework for addressing intermediate outcomes and is particularly attractive for applications with death truncation. This framework focuses on the always-survivor subgroup defined by the combination of observed and missing potential outcomes for the terminal event. Suppose the time to the first event is of interest, an existing estimand is the survivor average causal effect (SACE) for a fixed time point  $t$ :  $\Pr(T_{i1}^1 < t \mid t < D_i^0, t < D_i^1) - \Pr(T_{i1}^0 < t \mid t < D_i^0, t < D_i^1)$ . This quantity allows us to circumvent the potential bias by focusing on the subpopulation of individuals who would always survive regardless of the assigned treatment, i.e., both the

first and second probability statements are conditioned on the same cohort of individuals. For example, Lyu et al. (2023) adopted this definition of the always-survivor and defined the SACE for recurrent events with a terminal event. In particular, they considered the causal contrast of the number of recurrent events defined as  $\mathbb{E}[N_i^1(t) - N_i^0(t) \mid t < D_i^0, t < D_i^1]$ .

Comment et al. (2019) argued that estimating the SACE at a single time point  $t$  may present certain challenges. This is because it describes causal effects only for the always-survivor subpopulation at that specific moment, which they call a snapshot effect. This static approach fails to account for the sensitivity to the choice of  $t$  because the focused subpopulation changes and diminishes over time, and thus overlooks how treatment effects accumulate or vary over time for a fixed subpopulation. Consequently, these snapshot estimands cannot capture the full temporal nature of treatment effects and fail to provide meaningful insights about the causal effects. Recent studies (e.g., Comment et al., 2019; Xu et al., 2022) have addressed this issue by focusing on double-indexed estimands, where the principal strata are defined by the time index  $r$ , independent of the choice of  $t$  that indexes the time to the events of interest. This approach introduces the time-varying SACE (TV-SACE), where the population of always-survivors depends only on the chosen time  $r$ , that is,  $\Pr(T_{i1}^1 < t \mid r < D_i^0, r < D_i^1) - \Pr(T_{i1}^0 < t \mid r < D_i^0, r < D_i^1)$ .

The double-index approach appears promising; however, it has potential limitations when applied to recurrent events. Specifically, the traditional definition  $\mathcal{AS}_{\text{trad}}(r) = \{i : r < D_i^0, r < D_i^1\}$  may unnecessarily exclude units from the always-survivor stratum when there is a large gap between the time of the last recurrent event and the cutoff time  $r$ . Figure 1 illustrates this phenomenon: units 1–4 are excluded from the always-survivor stratum according to the standard definition, despite surviving until the final recurrent event of interest. Consequently, the inference for the stratum may become unstable as the

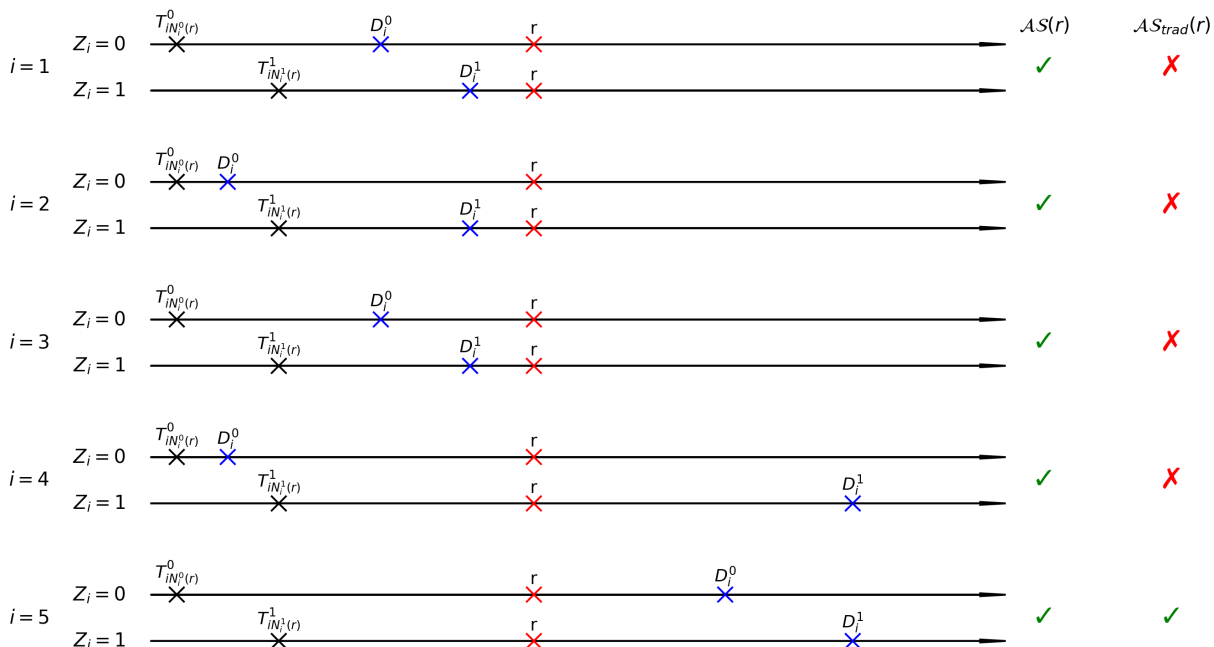


Figure 1: Illustration of different definitions of always-survivor strata in recurrent event analyses with terminal events. The traditional definition is given by  $\mathcal{AS}_{\text{trad}}(r) = \{i : r < D_i^0, r < D_i^1\}$ . Under our definition, units 1-5 belong to the always-survivor stratum, while the traditional definition excludes units 1-4, classifying only unit 5 as an always-survivor.

stratum size becomes smaller. Additionally, as  $r$  increases, the subpopulation of always-survivors eventually diminishes and may even be empty. These limitations motivate us to consider alternative definitions of the always-survivor subpopulation in the context of recurrent events.

Specifically, we propose a partition based on the ordering of the terminal event outcome and the non-terminal recurrent event outcome, for a fixed time point  $r$  with  $t < r$ . We define the always-survivor stratum at time  $r$  as  $\mathcal{AS}(r) = \{i : T_{iN_i^1(r)}^1 < D_i^1, T_{iN_i^0(r)}^0 < D_i^0\}$ , which consists of individuals for whom the  $N_i^z(r)$ -th recurrent event occurs before the terminal event under both treatment and control. The never-survivor stratum is defined as  $\mathcal{NS}(r) = \{i : T_{iN_i^1(r)}^1 = *, T_{iN_i^0(r)}^0 = *\}$ , indicating individuals for whom the  $N_i^z(r)$ -th recurrent event would have occurred only after the terminal event under both treatment and control, and is therefore undefined as a pre-death recurrent event. See Table 1 for the

Table 1: Stratification based on the recurrent event and terminal event.

Name	Stratum definition
Always-survivor ( $\mathcal{AS}(r)$ )	$T_{iN_i^0(r)}^0 < D_i^0$ & $T_{iN_i^1(r)}^1 < D_i^1$
Never-survivor ( $\mathcal{NS}(r)$ )	$T_{iN_i^0(r)}^0 = *$ & $T_{iN_i^1(r)}^1 = *$
Survival-harmed ( $\mathcal{SH}(r)$ )	$T_{iN_i^0(r)}^0 = *$ & $T_{iN_i^1(r)}^1 < D_i^1$
Survival-protected ( $\mathcal{SP}(r)$ )	$T_{iN_i^0(r)}^0 < D_i^0$ & $T_{iN_i^1(r)}^1 = *$

definitions of the remaining two strata. Similar ideas can be found in Nevo and Gorfine (2022); Yu et al. (2024); Zehavi et al. (2025), but their strata are defined for non-recurrent time-to-event. Note that our definition of the always-survivor stratum circumvents the aforementioned issue that it becomes scarce or even empty as time grows by considering survivorship at the exact time when the final recurrent event occurs before a prefixed time  $r$ . Even when the gap between the final recurrent event and the fixed time  $r$  is large, our definition of strata is robust to the choice of  $r$ , providing a more time-stable subgroup of survival units tailored for unique features of recurrent events. Figure 1 illustrates the difference between our approach and the conventional approach (e.g., Lyu et al., 2023) in defining always-survivors.

## 2.2 Principal stratum causal estimands

Our interest lies in evaluating the causal effect on the recurrent event process for always-survivors in Table 1, which is relevant when  $N_i^z(\cdot)$  and  $T_{ij}^z$  can be undefined due to truncation. We first define the *survivor-average number of recurrence* (SANR) estimands as

$$\text{SANR}(t; r) = g\{\mu^1(t; r), \mu^0(t; r)\}, \quad (1)$$

where  $\mu^z(t; r) = \mathbb{E}[N_i^z(t) \mid \mathcal{AS}(r)]$  for  $t < r$ . The function  $g(\cdot, \cdot)$  determines the scale of effect measure. For example,  $g(x, y) = x - y$  and  $g(x, y) = x/y$  correspond to causal

mean difference and causal rate ratio, respectively. These class of estimands represent the causal contrast in the number of event occurrences before time  $t$ . The second class of estimands pertain to the *event rate* among always-survivors, thereby answering the question of how many recurrent events we expect per unit time alive under each treatment arm. For the principal stratum  $\mathcal{AS}(r)$  we define  $\tau^z(t; r) = \mathbb{E}[T_{iN_i^z(t)}^z \mid \mathcal{AS}(r)]$ , so that the ratio  $\mu^z(t; r)/\tau^z(t; r)$  represents the average number of events per unit exposure time for an always-survivor in arm  $z$ . We formalize the *survivor-average event-rate* (SAER) estimands as

$$\text{SAER}(t; r) = g\left\{\frac{\mu^1(t; r)}{\tau^1(t; r)}, \frac{\mu^0(t; r)}{\tau^0(t; r)}\right\}. \quad (2)$$

$\text{SAER}(t; r) < 1$  indicates that, per person-year alive, the treatment reduces the expected number of events relative to control, whereas a value above one indicates the opposite. The SAER estimand quantifies how many events are caused per unit follow-up, providing a direct public-health interpretation in terms of event occurrences per person-year. A more detailed discussion on the SAER is provided in Web Appendix A.

### 3 Bayesian Nonparametric Causal Inference

Leveraging Bayesian methods for causal inference, we first consider the joint distribution of all potential variables and covariates  $(\mathbf{N}^0(\cdot), \mathbf{D}^0, \mathbf{C}^0, \mathbf{N}^1(\cdot), \mathbf{D}^1, \mathbf{C}^1, \mathbf{X}, \mathbf{Z})$ . We assume that the parameters governing the distribution of  $\mathbf{C}^z$ ,  $\mathbf{Z}$  and  $\mathbf{X}$  is a priori independent of the parameters of  $\mathbf{N}^z(\cdot)$  and  $\mathbf{D}^z$ . Under Assumption 3 and the prior independence, the censoring variables do not affect the inference of the quantities of scientific interest (e.g., Rubin (1978)), thus we focus on the joint distribution of  $(\mathbf{N}^0(\cdot), \mathbf{D}^0, \mathbf{N}^1(\cdot), \mathbf{D}^1, \mathbf{Z}, \mathbf{X})$ . Assuming unit exchangeability, the de Finetti's theorem implies the existence of parameters

such that

$$\begin{aligned}
& p(\mathbf{N}^0(\cdot), \mathbf{D}^0, \mathbf{N}^1(\cdot), \mathbf{D}^1, \mathbf{Z}, \mathbf{X}) \\
&= \int_{\Theta} p(\boldsymbol{\theta}^*) p(\boldsymbol{\varphi}^*) \prod_{i=1}^n p(N_i^0(\cdot) D_i^0, N_i^1(\cdot), D_i^1 \mid \mathbf{X}_i, \boldsymbol{\theta}^*) p(Z_i, \mathbf{X}_i \mid \boldsymbol{\varphi}^*) d\boldsymbol{\theta}^* d\boldsymbol{\varphi}^*,
\end{aligned} \tag{3}$$

where the global parameter  $\boldsymbol{\theta}^*$  has prior  $p(\boldsymbol{\theta}^*)$ . Under the ignorable treatment assignment (Assumption 2), the assignment model does not affect the inference of the quantities of scientific interest  $\boldsymbol{\theta}^*$  either. In what follows, we will conduct a likelihood analysis for  $\boldsymbol{\theta}^*$ , assuming that the value of  $\boldsymbol{\theta}^*$  which governed the distribution of observable data has been drawn from a prior distribution with compact support. For identification, we further assume that a *frailty*  $\boldsymbol{\gamma}$  is included as unknown parameters in an expanded parameter set  $\boldsymbol{\theta}^* = (\boldsymbol{\theta}, \boldsymbol{\gamma})$  for  $\boldsymbol{\gamma} = (\gamma_1, \dots, \gamma_n)^\top$ , as formalized below.

**Assumption 4** (Cross-world conditional independence). *For each unit  $i$ , there exists a bivariate frailty  $\boldsymbol{\gamma}_i = (\gamma_i^0, \gamma_i^1)$  such that the joint distribution of the potential outcomes is factorized:  $p(N_i^0(\cdot), D_i^0, N_i^1(\cdot), D_i^1 \mid \mathbf{X}_i, \boldsymbol{\gamma}_i) = p(N_i^0(\cdot), D_i^0 \mid \mathbf{X}_i, \gamma_i^0) p(N_i^1(\cdot), D_i^1 \mid \mathbf{X}_i, \gamma_i^1)$ .*

The frailty device has been previously considered in the semi-competing risks literature (e.g., Stensrud et al., 2017; Comment et al., 2019; Nevo and Gorfine, 2022; Lyu et al., 2023). Here, the individual frailty  $\boldsymbol{\gamma}_i$  governs two distinct forms of dependence: (i) *cross-world* dependence between treatment arms, arising from the association between  $\gamma_i^0$  and  $\gamma_i^1$ ; and (ii) *within-world* dependence between the terminal event  $D_i^z$  and the recurrent event process  $N_i^z(\cdot)$  under treatment  $z$ . A popular simplification sets  $\gamma_i^0 = \gamma_i^1 \equiv \gamma_i$ . Although this assumption conveniently captures within-world dependence between recurrent events and the terminal event in descriptive (non-causal) analyses (e.g., Paulon et al., 2020; Tian et al., 2024), in causal analyses it also imposes the same dependence structure between cross-worlds, thereby yielding point identification of the causal contrasts. (e.g., Comment et al.,

2019; Lyu et al., 2023). Because this within-world dependence shared across different worlds rarely holds unless all effect modifiers are measured and modeled correctly, this approach imposes strong, and often opaque, assumptions on dependence structures in causal settings.

Similar to Nevo and Gorfine (2022) who addressed the non-recurrent event setting, we retain separate frailties  $\gamma_i^0$  and  $\gamma_i^1$  and introduce a sensitivity parameter  $\rho = \text{Corr}(\gamma_i^0, \gamma_i^1)$  that captures their cross-world association. This formulation separates identifiable and non-identifiable components: the marginal distributions of  $\gamma_i^0$  and  $\gamma_i^1$ , and hence the within-world dependence, are estimable from the observed data, whereas the cross-world correlation  $\rho$  is an unidentifiable, cross-world quantity. Nevo and Gorfine (2022) specified a correlated gamma distribution for the joint frailty, fixing the location parameters and correlation parameter  $\rho$  *a priori* and thereby constraining the model to a relatively restrictive parametric family. We consider a sensitivity analysis framework by placing a flexible non-parametric prior on the joint distribution of  $(\gamma_i^0, \gamma_i^1)$  conditional on a fixed  $\rho$ , specified in Section 3.1.2. Sensitivity analysis is carried out by varying  $\rho$  and examining how posterior estimates of the causal estimands change, as illustrated in Section 5.

Assumption 4 allows us to derive the posterior distribution of  $\boldsymbol{\theta}^* = (\boldsymbol{\theta}, \boldsymbol{\gamma})$  as

$$p(\boldsymbol{\theta}, \boldsymbol{\gamma} \mid \mathbf{N}^{\text{obs}}(\cdot), \mathbf{D}^{\text{obs}}, \mathbf{Z}, \mathbf{X}) \propto p(\boldsymbol{\theta}, \boldsymbol{\gamma}) \prod_{i=1}^n p(N_i(\cdot), D_i \mid Z_i, \mathbf{X}_i, \boldsymbol{\theta}, \gamma_i^{Z_i}), \quad (4)$$

where the vectors with the superscript ‘obs’ denote the observed vectors of each potential outcome. To obtain the posterior distribution of the causal estimands, we then specify priors of  $\boldsymbol{\theta}$  and  $\boldsymbol{\gamma}$  and the likelihood for (4) and impute each unit’s missing potential outcomes by sampling from their posterior predictive distribution,  $p(N_i^{1-Z_i}(\cdot), D_i^{1-Z_i} \mid Z_i, \mathbf{X}_i, \boldsymbol{\theta}, \gamma_i^{1-Z_i})$ . Theorem 1 states that (1) is identifiable up to the frailty  $\boldsymbol{\gamma}$ .

**Theorem 1.** *Under Assumptions 1 – 4, (1) and (2) are nonparametrically identified up to*

distribution of the frailty  $\gamma$  as follows:

$$\begin{aligned}\mu^z(t; z) &= \frac{\int_{\mathcal{X}} \int_0^\infty \kappa_{t,r}(z, x, \gamma) \eta_r(1, x, \gamma) \eta_r(0, x, \gamma) f_\gamma(\gamma) f_X(x) d\gamma dx}{\int_{\mathcal{X}} \int_0^\infty \eta_r(1, x, \gamma) \eta_r(0, x, \gamma) f_\gamma(\gamma') f_X(x') d\gamma' dx'}, \\ \tau^z(t; r) &= \frac{\int_{\mathcal{X}} \int_0^\infty \zeta_{t,r}(z, x, \gamma) \eta_r(1, x, \gamma) \eta_r(0, x, \gamma) f_\gamma(\gamma) f_X(x) d\gamma dx}{\int_{\mathcal{X}} \int_0^\infty \eta_r(1, x, \gamma) \eta_r(0, x, \gamma) f_\gamma(\gamma') f_X(x') d\gamma' dx'},\end{aligned}\tag{5}$$

where  $\kappa_{t,r}(z, x, \gamma) = \mathbb{E}[N_i(t) \mid Z_i = z, T_{iN_i(r)} < D_i, \mathbf{X}_i = \mathbf{x}, \gamma]$ ,  $\zeta_{t,r}(z, x, \gamma) = \mathbb{E}[T_{iN_i(t)} \mid Z_i = z, T_{iN_i(r)} < D_i, \mathbf{X}_i = \mathbf{x}, \gamma]$ , and  $\eta_r(z, x, \gamma) = \Pr(T_{iN_i(r)} < D_i \mid Z_i = z, \mathbf{X}_i = \mathbf{x}, \gamma)$ .

The proof is provided in Web Appendix C. Theorem 1 motivates a g-computation strategy for estimating the target estimand based on observed data. This result clarifies that the correlation parameter  $\rho$  is not identifiable, which in turn suggests a sensitivity framework for posterior inference. We detail the specification of the working models in Section 3.1.

### 3.1 BNP for principal stratification with recurrent events truncated by a terminal event

#### 3.1.1 Enriched dependent Dirichlet process

Although Bayesian causal inference based on Theorem 1 can proceed with parametric models for recurrent events and the terminal event, the resulting causal estimators may be prone to model misspecification bias. To mitigate such bias, flexible model specifications, and particularly, Bayesian nonparametric (BNP) methods represent an attractive approach that can better adapt to a wider class of data.

A popular BNP approach for recurrent processes with a terminal event is jointly modeling the gap times of recurrent and terminal events using a Dirichlet process (DP) mixture model. While this is a simple approach adopted in the literature for the joint analysis of

recurrent events with a terminal event (Paulon et al., 2020; Xu et al., 2022; Tian et al., 2024), a potential pitfall is that the latent random partition induced by the DP will be overwhelmingly determined by the recurrent events rather than the terminal event as the number of recurrences grows, leading to unreliable within-cluster predictions of the survival time, with higher posterior variance due to unnecessarily small sample sizes. Additionally, existing approaches use the joint DP primarily to model a frailty term, but it is somewhat counterintuitive that the random partition, which yields the subject-specific frailty, is driven largely by numerous recurrent events rather than the subject-specific survival event. More technical discussions on this partitioning issue are provided in Web Appendix B.

We address these issues by introducing a nested structure into the DP prior tailored for the analysis of recurrent events with semi-competing risks. The key idea is to introduce a nested partition for the unknown random joint probability measure  $\mathbf{P}$ . In particular, we consider the random marginal  $\mathbf{P}_\phi$  and the random conditional  $\mathbf{P}_{\theta|\phi}$  to obtain the desired clustering structure. Then, the nested prior is defined as  $\mathbf{P}_\phi \sim \text{DP}(\alpha_\phi, P_{0\phi})$ ,  $\mathbf{P}_{\theta|\phi} \sim \text{DP}(\alpha_\theta(\phi), P_{0\theta|\phi}(\cdot | \phi))$  for all  $\phi \in \Phi$ , where  $\mathbf{P}_{\theta|\phi}$  for  $\phi \in \Phi$  are independent of  $\mathbf{P}_\phi$ . These assumptions induce a prior for the random joint distribution  $\mathbf{P}$  through the joint law of the marginal and conditionals and the mapping  $(P_\phi, P_{\theta|\phi}) \rightarrow \int P_{\theta|\phi}(\cdot | \phi) dP_\phi$ . Then, the prior is parameterized by the base measure  $P_0$ , defined by  $P_0(A \times B) = \int_A P_{\theta|\phi}(B | \phi) dP_\phi$ . This nested prior structure is called the *Enriched Dirichlet process (EDP)* prior (Wade et al., 2011).

One core assumption of the EDP is that the distributions are exchangeable at both survival and recurrent event levels. However, in practice, we often have access to subject-specific covariates  $\mathbf{X}_i$  and time-varying covariates  $\mathbf{V}_{ij}$  at the  $j$ -th recurrence. These variables provide useful information in characterizing the distributions at both levels, and we

hence further incorporate the dependence of the covariates on the EDP through the use of the dependent Dirichlet process (DDP) (Maceachern, 1999) to relax the exchangeability assumption. We refer to the resulting prior as the *enriched dependent Dirichlet process* (EDDP). The enriched dependent Dirichlet process mixture (EDDPM) uses the EDDP as a prior for the mixing distribution. The key idea behind the EDDP is to define a set of random measures that are marginally EDP-distributed for every possible combination of covariates  $\mathbf{x}$  and  $\mathbf{v}$ . Using a square-breaking construction of the EDP (Wade et al., 2011), the density associated with the EDDP is

$$f(u, \bar{y} | P) = \sum_{k=1}^{\infty} \sum_{l=1}^{\infty} w_k^{\phi} w_{l|k}^{\theta} K(u | \bar{y}, \phi_k(\mathbf{x})) K(\bar{y} | \theta_{l|k}(\mathbf{x}, \mathbf{v})) \quad (6)$$

where  $w_k^{\phi} = v_k^{\phi} \prod_{l < k} (1 - v_l^{\phi})$ ,  $v_k^{\phi} \sim \text{Beta}(1, \alpha_{\phi})$  with  $w_1^{\phi} = v_1^{\phi}$ ,  $w_{l|k}^{\theta} = v_{l|k}^{\theta} \prod_{j < l} (1 - v_{j|k}^{\theta})$ ,  $v_{l|k}^{\theta} \sim \text{Beta}(1, \alpha_{\theta}(\phi))$  with  $w_{1|k}^{\theta} = v_{1|k}^{\theta}$  for each  $k$ , and  $\phi_k(\mathbf{x}) \sim P_{0\phi}^{\mathbf{x}}$ ,  $\theta_l(\mathbf{x}, \mathbf{v}) \sim P_{0\theta|\phi}^{\mathbf{x}, \mathbf{v}}$ .  $\phi_k(\mathbf{x})$  and  $\theta_{l|k}(\mathbf{x}, \mathbf{v})$  are stochastic processes drawn independently from marginal distributions  $P_{\phi}^{\mathbf{x}}$  and  $P_{0\theta|\phi}^{\mathbf{x}, \mathbf{v}}(\cdot | \phi)$ , indexed by the baseline and time-varying covariates  $\mathbf{x}$  and  $\mathbf{v}$ . This construction corresponds to the *single-weights* DDP model (Maceachern, 1999), where the atom processes are indexed by covariates, but the weights are independent of the covariates.

### 3.1.2 Model specifications

For  $i = 1, \dots, n$  and  $j = 1, \dots, N_i$ , the log-scale survival time  $U_i$  and  $j$ -th recurrent gap time  $Y_{ij}$  are specified by the following hierarchical model.

$$\begin{aligned}
U_i \mid Z_i = z, \mathbf{X}_i = \mathbf{x} &\sim K_u(\boldsymbol{\phi}_i(\mathbf{x}, z)) \equiv \text{N}((\mathbf{x}, z)\boldsymbol{\beta}_{u,i} + \gamma_i^z, \tau_i^2), \\
Y_{ij} \mid Z_i = z, \mathbf{X}_i = \mathbf{x}, \mathbf{V}_{ij} = \mathbf{v} &\sim K_y(\boldsymbol{\theta}_{ij}(\mathbf{x}, \mathbf{v}, z)) \equiv \text{N}((\mathbf{x}, \mathbf{v}, z)\boldsymbol{\beta}_{y,ij} + \psi_{ij}\gamma_i^z, \sigma_{ij}^2), \\
\boldsymbol{\phi}_i(\mathbf{x}, z) &\sim P_\phi^\mathbf{x}, \quad P_\phi^\mathbf{x} \sim \text{DP}(\alpha_\phi, P_{0\phi}^\mathbf{x}) \\
\boldsymbol{\theta}_{ij}(\mathbf{x}, \mathbf{v}, z) &\sim P_{\theta|\phi}^{\mathbf{x},\mathbf{v}}, \quad P_{\theta|\phi}^{\mathbf{x},\mathbf{v}} \sim \text{DP}(\alpha_{\theta|\phi}(\phi), P_{0\theta|\phi}^{\mathbf{x},\mathbf{v}}(\cdot \mid \phi)),
\end{aligned} \tag{7}$$

where the atom processes are expressed by simple linear models and variance parameters:

$\boldsymbol{\phi}_i(\mathbf{x}, z) = ((\mathbf{x}, z)\boldsymbol{\beta}_{u,i}, \gamma_i, \tau_i)$  and  $\boldsymbol{\theta}_{ij}(\mathbf{x}, \mathbf{v}, z) = ((\mathbf{x}, \mathbf{v}, z)\boldsymbol{\beta}_{y,ij}, \psi_{ij}, \sigma_{ij}, \gamma_i)$ . Additionally, we

assume  $\alpha_\phi \sim \text{Ga}(a_{\alpha_\phi}, b_{\alpha_\phi})$ ,  $\alpha_{\theta|\phi}(\phi) = \alpha_{\theta|\phi} \sim \text{Ga}(a_{\alpha_{\theta|\phi}}, b_{\alpha_{\theta|\phi}})$ , and the marginal base mea-

asures are  $P_{0\phi}^\mathbf{x} = \text{MVN}(\boldsymbol{\mu}_{\beta_u}, \boldsymbol{\Sigma}_{\beta_u})\text{MVN}(\boldsymbol{\mu}_\gamma, \boldsymbol{\Sigma}_\gamma)\text{IG}(a_\tau, b_\tau)$ , where  $\boldsymbol{\Sigma}_\gamma = \begin{pmatrix} \sigma_{\gamma_0}^2 & \rho\sigma_{\gamma_0}\sigma_{\gamma_1} \\ \rho\sigma_{\gamma_0}\sigma_{\gamma_1} & \sigma_{\gamma_1}^2 \end{pmatrix}$

with a given correlation parameter  $\rho$ , and  $P_{0\theta|\phi}^{\mathbf{x},\mathbf{v}}(\cdot \mid \phi) = \text{MVN}(\boldsymbol{\mu}_{\beta_y}, \boldsymbol{\Sigma}_{\beta_y})\text{N}(\mu_\psi, \sigma_\psi^2)\text{IG}(a_\sigma, b_\sigma)\delta_\gamma$ ,

with  $\delta_\gamma$  being a dirac measure centered on  $\boldsymbol{\gamma} = (\gamma_1, \dots, \gamma_n)$ . We will discuss specific choices

of the hyperparameters of each prior in the simulation studies and empirical analyses.

The hierarchical model (7) is equivalent to jointly modeling the observed recurrent gap times and survival time for each unit through the infinite mixture of the log-normal kernels. It is worth mentioning that many existing approaches to the analysis of recurrent and survival events in non-causal analyses only place a DP prior on the random frailty of a linear model and/or the residuals. While their model relaxes the distributional assumption on the random effects in the linear model, it still makes strong structural assumptions about how the parametric fixed effects are correlated with the outcome (i.e., linearity assumption). In contrast, our model is intrinsically functional, placing EDDPM priors on the functional space of the survival and recurrent event models.

Another salient feature of the proposed EDDPM for recurrent–terminal event data is its treatment of the subject-specific frailty vector  $\boldsymbol{\gamma}_i = (\gamma_i^0, \gamma_i^1)$ . We first sample  $\boldsymbol{\gamma}_i$  from the first-level marginal base measure  $P_{0\phi}^{\mathbf{x}}$ , which governs the terminal-event distribution, and then propagate this same value through the second-level conditional base measure  $P_{0\theta|\phi}^{\mathbf{x},\mathbf{v}}(\cdot | \phi) \propto \delta_{\boldsymbol{\gamma}_i}$ , so that the nested EDDP prior carries identical frailty information into the recurrent gap-time model. The frailty  $\boldsymbol{\gamma}_i$  captures unobserved heterogeneity for the terminal event, while the parameters  $\psi_{ij}$  determine how this heterogeneity modifies each recurrent gap time for subject  $i$ . This nested construction avoids the unfavorable random-partition behavior highlighted in Section 3.1 (see also Section 3.1.3). Conditional on  $\boldsymbol{\gamma}_i$  we assume independence between the terminal event and the recurrent events, a standard simplifying device in descriptive analyses of such data (Paulon et al., 2020; Xu et al., 2021; Tian et al., 2024). Additionally, to express the potential cross-world dependence, we take the base measure of  $\boldsymbol{\gamma}_i$  to be  $\text{MVN}(\boldsymbol{\mu}_\gamma, \boldsymbol{\Sigma}_\gamma)$ , where  $\boldsymbol{\Sigma}_\gamma = \begin{pmatrix} \sigma_{\gamma_0}^2 & \rho\sigma_{\gamma_0}\sigma_{\gamma_1} \\ \rho\sigma_{\gamma_0}\sigma_{\gamma_1} & \sigma_{\gamma_1}^2 \end{pmatrix}$ . The non-identifiable correlation between the cross-world frailties  $\gamma_i^0$  and  $\gamma_i^1$  is captured by a sensitivity parameter  $\rho$ , which induces the dependence structure between  $\gamma_i^0$  and  $\gamma_i^1$ , and hence the observed and missing potential outcomes. Although we fix  $\rho$  when fitting the model, our empirical study demonstrates how varying this parameter facilitates a principled sensitivity analysis. Overall, this formulation allows for a flexible, nonparametric characterization of the survival event distribution, while still permitting subject-level random effects  $\boldsymbol{\gamma}_i$  that may be correlated with recurrent gap times through  $\psi_{ij}\boldsymbol{\gamma}_i$ .

### 3.1.3 Random partition properties

When applied to recurrent event data with a terminal event, the standard DP induces a random partition that is predominantly determined by the recurrent events rather than the terminal event. We provide detailed discussions on this unfavorable property of the DP-

induced partition in Web Appendix B.2. This section discusses how the random partition induced by our proposed prior addresses this limitation. Define  $\mathcal{P}_n = (\mathcal{P}_{n,u}, \mathcal{P}_{n,y})$ , where  $\mathcal{P}_{n,u} = (s_{u,1}, \dots, s_{u,n})$  and  $\mathcal{P}_{n,y} = (s_{y,1}, \dots, s_{y,n})$  denote random partitions defined by cluster allocation labels. Specifically,  $s_{u,i} = j$  if  $\phi_i = \phi_j^*$  is the  $j$ -th distinct value of the atom  $\phi$ , and  $s_{y,i} = l$  if  $\theta_i = \theta_{l|j}^*$  is the  $l$ -th distinct value of the atom  $\theta$  within the  $j$ -th  $\phi$ -cluster. For each  $\phi$ -cluster  $j$ , let  $\mathcal{S}_j = \{i : s_{u,i} = j\}$ , so  $n_j = |\mathcal{S}_j|$  is the number of individuals in the  $j$ -th  $\phi$ -cluster. Denote the total number of  $\phi$ -clusters by  $M_n$ . Within each  $\phi$ -cluster  $j$ , define  $\mathcal{S}_{l|j} = \{i : s_{u,i} = j, s_{y,i} = l\}$ , so  $n_{l|j} = |\mathcal{S}_{l|j}|$  is the size of the  $l$ -th  $\theta$ -subcluster, and let  $M_{n,j}$  be the number of  $\theta$ -subclusters within cluster  $j$ . The unique cluster-specific parameters are then  $\phi^* = (\phi_j^*)_{j=1}^{M_n}$  and  $\theta^* = (\theta_{1|j}^*, \dots, \theta_{M_{n,j}|j}^*)_{j=1}^{M_n}$ . Finally, define  $\mathcal{P}_{n,y} = (s_{y,i} : i \in \mathcal{S}_j)$ ,  $U_j^* = \{U_i : i \in \mathcal{S}_j\}$ ,  $\bar{Y}_j^* = \{\bar{Y}_i : i \in \mathcal{S}_j\}$ ,  $\bar{Y}_{l|j}^* = \{\bar{Y}_i : i \in \mathcal{S}_{l|j}\}$ .

Consider the joint posterior distribution of the partition and the cluster parameters:

$$p(\mathcal{P}_n, \phi^*, \theta^* \mid \bar{Y}_{1:n}, U_{1:n}) \propto p(\mathcal{P}_n) \prod_{j=1}^{M_n} p_{0\phi}(\phi_j^*) \prod_{l=1}^{M_{n,j}} p_{0\theta}(\theta_{l|j}^*) \prod_{j=1}^{M_n} \prod_{i \in \mathcal{S}_j} K(U_i \mid \bar{Y}_i, \phi_j^*) \prod_{l=1}^{M_{n,j}} \prod_{i \in \mathcal{S}_{l|j}} K(\bar{Y}_i \mid \theta_{l|j}^*).$$

The posterior distributions of the cluster-specific parameters are

$$\begin{aligned} p(\phi_j^* \mid \mathcal{P}_n, \bar{Y}_{1:n}, U_{1:n}) &\propto p_{0\phi}(\phi_j^*) \prod_{i \in \mathcal{S}_j} K(U_i \mid \bar{Y}_i, \phi_j^*), \\ p(\theta_{l|j}^* \mid \mathcal{P}_n, \bar{Y}_{1:n}, U_{1:n}) &\propto p_{0\theta}(\theta_{l|j}^*) \prod_{i \in \mathcal{S}_{l|j}} K(\bar{Y}_i \mid \theta_{l|j}^*). \end{aligned} \tag{8}$$

The EDP random partition is further characterized by the following proposition.

**Proposition 1.** *The prior on the random partition induced by the EDP is*

$$p(\mathcal{P}_n) = \frac{\Gamma(\alpha_\phi)}{\Gamma(\alpha_\phi + n)} \alpha_\phi^{M_n} \prod_{j=1}^{M_n} \int_{\Phi} \alpha_\theta(\phi)^{M_{n,j}} \frac{\Gamma(\alpha_\theta(\phi)) \Gamma(n_j)}{\Gamma(\alpha_\theta(\phi) + n_j)} dP_{0\phi}(\phi) \prod_{l=1}^{M_{n,j}} \Gamma(n_{l|j}).$$

Furthermore, the posterior of the random partition of the EDP model is

$$p(\mathcal{P}_n | \bar{Y}_{1:n}, U_{1:n}) \propto \alpha_\phi^{M_n} \prod_{j=1}^{M_n} \int_{\Phi} \alpha_\theta(\phi)^{M_{n,j}} \frac{\Gamma(\alpha_\theta(\phi))\Gamma(n_j)}{\Gamma(\alpha_\theta(\phi) + n_j)} dP_{0\phi}(\phi) h_u \left( U_j^* | \bar{Y}_j^* \right) \prod_{l=1}^{M_{n,j}} \Gamma(n_{l|j}) h_y \left( \bar{Y}_{l|j}^* \right), \quad (9)$$

where  $h_u \left( U_j^* | \bar{Y}_j^* \right) = \int_{\Phi} \prod_{i \in \mathcal{S}_j} K \left( U_i | \bar{Y}_i, \phi \right) dP_{0\phi}(\phi)$  and  $h_y \left( \bar{Y}_{l|j}^* \right) = \int_{\Theta} \prod_{i \in \mathcal{S}_{l|j}} K \left( \bar{Y}_i | \theta \right) dP_{0\theta}(\theta)$ .

The proof is provided in Web Appendix C. Moreover, by marginalizing over all possible  $\theta$ -subpartitions for each  $\phi$ -cluster, one obtains the posterior for  $\mathcal{P}_{n,u}$ :

$$p(\mathcal{P}_{n,u} | \bar{Y}_{1:n}, U_{1:n}) \propto \alpha_\phi^{M_n} \prod_{j=1}^{M_n} h_u \left( U_j^* | \bar{Y}_j^* \right) \times \sum_{\mathcal{P}_{n_j,y} \in \Pi_{n_j}} \int_{\Phi} \alpha_\theta(\phi)^{M_{n,j}} \frac{\Gamma(\alpha_\theta(\phi))\Gamma(n_j)}{\Gamma(\alpha_\theta(\phi) + n_j)} dP_{0\phi}(\phi) \prod_{l=1}^{M_{n,j}} \Gamma(n_{l|j}) h_y \left( \bar{Y}_{l|j}^* \right), \quad (10)$$

where  $\Pi_{n_j}$  denotes the set of all possible partitions of  $n_j$  integers. The posterior (10) shows that  $\phi$ -clusters favored under the EDP are those in which individuals share a similar survival-recurrence relationship (reflected in  $h_u$ ), while finer distinctions among recurrent outcomes (captured by a mixture of the kernel of  $h_y$ ) appear as nested  $\theta$ -subclusters.

The posterior distributions (9) and (10) both reflect the desirable random-partition structure of the EDP. In particular, the nested framework separates the likelihood contributions from  $U_j^*$  (the survival component for individuals in the  $j$ -th  $\phi$ -cluster) and  $\bar{Y}_{l|j}^*$  (the recurrent events for individuals in the  $l$ -th  $\theta$ -subcluster within cluster  $j$ ). Hence, even when the data indicate that many  $\theta$ -subclusters are needed to capture fine differences in the recurrence process, these subclusters all remain nested under the coarser  $\phi$ -cluster. As a result, the number of top-level  $\phi$ -clusters,  $M_n$ , tends to remain modest, yielding a larger effective sample size  $n_j$  within each  $\phi$ -cluster. From (8), we see that  $\phi_j^*$  is updated using all  $U_i$  and  $\bar{Y}_i$  data in  $\mathcal{S}_j$ , regardless of how the cluster is further subdivided. This more

substantial pool of observations stabilizes posterior estimates of  $\phi_j^*$ .

### 3.1.4 Posterior inference

We develop a fully tractable Gibbs sampling algorithm for the posterior inference. First, the observed-data likelihood is given by:

$$\begin{aligned} \mathcal{L}_{\text{obs}} &= \prod_{i=1}^n f^{1-\delta_i^C} (U_i \mid Z_i, \mathbf{X}_i, \boldsymbol{\beta}_{u,i}, \gamma_i^{Z_i}, \tau_i) S_U^{\delta_i^C} (\log(\mathcal{T}_i) \mid Z_i, \mathbf{X}_i, \boldsymbol{\beta}_{u,i}, \gamma_i^{Z_i}, \tau_i) \\ &\quad \times \prod_{j=1}^{N_i} f(Y_{ij} \mid Z_i, \mathbf{X}_i, \mathbf{V}_{i(N_i+1)}, \boldsymbol{\beta}_{y,ij}, \psi_{ij}, \gamma_i^{Z_i}, \sigma_{ij}) \\ &\quad \times S_Y (\log(\mathcal{T}_i - T_{iN_i}) \mid Z_i, \mathbf{X}_i, \mathbf{V}_{i(N_i+1)}, \boldsymbol{\beta}_{y,i(N_i+1)}, \psi_{i(N_i+1)}, \gamma_i^{Z_i}, \sigma_{i(N_i+1)}), \end{aligned}$$

where  $S_Y$  and  $S_U$  denote the survival functions for  $Y$  and  $U$ , respectively. To facilitate the posterior inference based on the data augmentation, we consider the following complete data likelihood with truncated outcomes imputed.

$$\begin{aligned} \mathcal{L}_{\text{comp}} &= \prod_{i=1}^n f^{1-\delta_i^C} (U_i \mid Z_i, \mathbf{X}_i, \boldsymbol{\beta}_{u,i}, \gamma_i^{Z_i}, \tau_i) f^{\delta_i^C} (U_i^* \mid Z_i, \mathbf{X}_i, \boldsymbol{\beta}_{u,i}, \gamma_i^{Z_i}, \tau_i) \\ &\quad \times \prod_{j=1}^{N_i} f(Y_{ij} \mid Z_i, \mathbf{X}_i, \mathbf{V}_{ij}, \boldsymbol{\beta}_{y,ij}, \psi_{ij}, \gamma_i^{Z_i}, \sigma_{ij}) \\ &\quad \times f(Y_{i(N_i+1)}^* \mid Z_i, \mathbf{X}_i, \mathbf{V}_{i(N_i+1)}, \boldsymbol{\beta}_{y,i(N_i+1)}, \psi_{i(N_i+1)}, \gamma_i^{Z_i}, \sigma_{i(N_i+1)}), \end{aligned}$$

where  $Y^*$  and  $U^*$  represent the imputed values of the gap time and survival time, respectively. This complete likelihood admits the standard posterior sampling technique based on the densities. Specifically, we employ an approximated blocked Gibbs sampler based on a two-level truncation of the square-breaking representation of the EDP proposed by Burns and Daniels (2023). In this algorithm, we first select conservative upper bounds on

the number of latent classes of the square-breaking representation of (6) as follows.

$$f(u, \bar{y} | P) = \sum_{k=1}^K \sum_{l=1}^L w_k^\phi w_{l|k}^\theta \text{N}(u | (\mathbf{x}, z)^\top \boldsymbol{\beta}_{u,k} + \gamma_k^z, \tau_k^2) \text{N}(\bar{y} | (\mathbf{x}, \mathbf{v}, z)^\top \boldsymbol{\beta}_{y,l|k} + \psi_{l|k} \gamma_k^z, \sigma_{l|k}^2)$$

Let  $G_i \in \{1, \dots, K\}$  and  $H_{ij} \in \{1, \dots, L\}$  denote the latent cluster indicators for individual  $i = 1, \dots, n$  and time  $j = 1, \dots, N_i$ . Our data augmentation algorithm further imputes these latent indicators in each iteration to facilitate the posterior updates of model parameters. Specifically, we specify Multinomial distributions  $G_i \sim \text{MN}(\mathbf{w}^\phi)$  on  $G_i$  and  $H_{ij} \sim \text{MN}(\mathbf{w}_k^\theta)$  on  $H_{ij}$ , where  $\mathbf{w}^\phi = (w_1^\phi, \dots, w_K^\phi)^\top$  and  $\mathbf{w}_k^\theta = (w_{1|k}^\theta, \dots, w_{L|k}^\theta)^\top$  contains the weights from the EDDP. Burns and Daniels (2023) demonstrated that an accurate approximation to the exact EDP is obtained as long as the truncation bound is sufficiently large. To ensure this, we ran several MCMC iterations with different values of  $K$  and  $L$  and increased them if all clusters were occupied. Overall, our algorithm iterates between drawing from the conditional distributions of censored outcomes, latent cluster indicators, and model parameters.

The essential Gibbs sampler is outlined as follows: (i) given all model parameters,  $G_i$  and  $H_i$ , sample  $Y_{i(N_i+1)}^*$  and  $U_i^*$ , (ii) given all model parameters,  $Y_{i(N_i+1)}^*$  and  $U_i^*$ , sample  $G_i$  and  $H_i$ , (iii) given  $Y_{i(N_i+1)}^*$ ,  $U_i^*$ ,  $G_i$  and  $H_i$ , sample all model parameters, and (iv) compute the estimands based on Theorem 1. Specifically, when imputing  $(N_i + 1)$ -th gap time  $Y_{i(N_i+1)}^*$  in the first step, we draw from its conditional predictive distribution  $p(Y | Y > \log(\mathcal{T}_i - T_{iN_i}), -)$ , where “ $-$ ” denotes the rest of relevant variables, as the final gap time is always censored at  $\mathcal{T}_i - T_{iN_i}$ , the actual gap time should be greater than the censored gap time. Similarly, for the unit with  $\delta_i^C = 1$ , its survival time  $U_i$  from the posterior predictive distribution, enabling us to determine if the unit belongs to  $\mathcal{AS}(r)$ . For the imputation of  $U_i$  with  $\delta_i^C = 1$ , we also draw from its conditional predictive distribution

$p(U \mid U > \log(\mathcal{T}_i - D_i), -)$  as the survival time is censored and its actual survival time should be greater than the observed one. When computing estimands in the last step, e.g.,  $\mu^z(t; z)$ , we approximate it with its empirical distribution. For example, the numerator of  $\mu^z(t; z)$  in Theorem 1 is approximated by  $\frac{1}{n} \sum_{i=1}^n \kappa_{t,r}(Z_i, X_i, \gamma_i) \eta_{t,r}(1, X_i, \gamma_i) \eta_{t,r}(0, X_i, \gamma_i)$ . This is a conventional approximation in the Bayesian paradigm (Li et al., 2023). See Web Appendix D for full details of the algorithm. The initial parameter values were randomly drawn from the prior distributions, and the posterior samples were obtained by running a chain for 5000 MCMC iterations after an initial 20000 burn-in iteration. Convergence was monitored by the trace plots, confirming that the chains had reached stationarity with good mixing.

## 4 Simulation Studies

In this section we examine the performance of the proposed methods through simulation studies. Specifically, we evaluate the frequentist properties of the proposed EDDP prior for estimating the key estimands  $\mu^z(t; r)$  and  $\tau^z(t; r)$  for  $z \in \{0, 1\}$ , with comparisons to methods commonly used in the recurrent event analysis: linear model (LM) (e.g., Comment et al., 2019; Lyu et al., 2023), Dirichlet process mixture (DPM) (e.g., Paulon et al., 2020; Tian et al., 2024), and dependent Dirichlet process mixture (DDPM) (e.g., Xu et al., 2022).

We simulate 100 datasets with  $n = 2000$  individuals and evaluate the bias and root mean square error (RMSE) of a point estimator (posterior mean), as well as the frequentist coverage probability (CP) and average length (AL) of the 95% central credible interval. The dataset is generated from the following mixture models with random seeds.

$U_i^z \sim \sum_{k=1}^3 w_k \text{N}(\alpha^u + \mathbf{X}_i^\top \phi_k + z\beta_k^u + \gamma_i^z, 0.2)$ ,  $Y_{ij}^z \sim \sum_{k=1}^3 \pi_k \text{N}(\alpha^y + \mathbf{X}_i^\top \theta_k + z\beta_k^y + \psi\gamma_i^z, 0.2)$ , where  $\mathbf{X}_i \sim \text{MVN}((0, 0, 0)^\top, I_3)$  with  $I_d$  is the identity matrix of dimension  $d$ ,  $Z_i \sim$

Bern(0.5),  $(w_1, w_2, w_3) = (0.3, 0.4, 0.3)$ ,  $(\pi_1, \pi_2, \pi_3) = (0.3, 0.4, 0.3)$ ,  $\alpha^u = 6.5$ ,  $\alpha^y = 5.0$ ,  $\phi_1 = (0.2, 0.15, -0.1)^\top$ ,  $\phi_2 = 0.5\phi_1$ ,  $\phi_3 = 0.3\phi_1$ ,  $\theta_1 = (0.15, 0.10, -0.05)^\top$ ,  $\theta_2 = 0.5\theta_1$ ,  $\theta_3 = 0.3\theta_1$ ,  $(\beta_1^u, \beta_2^u, \beta_3^u) = (-1.0, -0.5, -1.3)$ ,  $(\beta_1^y, \beta_2^y, \beta_3^y) = (-0.4, -0.2, -0.52)$ , and  $\psi = 0.1$ . The frailty follows the multivariate log-normal distribution such that  $\gamma_i = \exp(\gamma'_i)$ , where  $\gamma'_i \sim \text{MVN}((0, 0)^\top, \begin{pmatrix} 0.2 & 0.2\rho \\ 0.2\rho & 0.2 \end{pmatrix})$  with a correlation parameter  $\rho = 0.5$ . The mixture components  $w_k$  and  $\pi_k$  take the same weight value for  $k = 1, 2, 3$ , but the assignment to each distribution component is independent. The observed survival time and recurrent gap times are obtained by transforming the log-scale variables  $U_i^z$  and  $Y_{ij}^z$  into  $D_i = \exp(U_i^{Z_i})$  and  $T_{ij} = \exp(Y_{ij}^{Z_i})$ , and  $T_{ij}$  is generated recurrently until the sum exceeds the censoring time  $\mathcal{T}_i = \min(D_i, C_i)$  where  $C_i \sim \text{Unif}(300, 1000)$ , where  $C_i$  represents the independent censoring time for each individual. The estimands' true values are approximated by Monte Carlo simulation using large samples.

For inference, we use model (7) for the EDDPM. In the DDPM, the nested prior structure is removed from the EDDPM. In the DPM, covariate dependence is further removed from the DDPM, and the frailty and error terms are modeled using the DPM, resulting in a model equivalent to that of Paulon et al. (2020). For the LM, we fit a linear mixed model to the log-transformed survival and gap times. The specification includes a subject-level frailty term and assumes normal residual errors, which yields the familiar accelerated failure time (AFT) representation. This setup is close to the models explored by Comment et al. (2019); Lyu et al. (2023). The only difference is that their proportional hazard model assumes an extreme-value distribution for the error term. We use proper, weakly informative conjugate priors for all parameters. Specifically, we choose the hyperparameters  $a_{\alpha_\phi} = \alpha_{\theta|\phi} = a_\tau = a_\sigma = 2.0$ ,  $b_{\alpha_\phi} = b_{\alpha_{\theta|\phi}} = b_\tau = b_\sigma = 1.0$ ,  $\mu_\gamma = \mu_\psi = 0.0$ ,  $\sigma_\gamma^2 = \sigma_\psi^2 = 3.0^2$ ,  $\boldsymbol{\mu}_{\beta_u}$  and  $\boldsymbol{\mu}_{\beta_y}$  are zero-vectors of appropriate sizes, and  $\boldsymbol{\Sigma}_{\beta_u}$  and  $\boldsymbol{\Sigma}_{\beta_y}$  are diagonal matrices

Table 2: Bias and root mean squared error (RMSE) of point estimates, and coverage probability (CP) and average length (AL) of 95% central credible intervals of the key estimands.

Model	$\mu_{500}^0(500)$				$\mu_{500}^1(500)$				$\tau_{500}^0(500)$				$\tau_{500}^1(500)$			
	Bias	RMSE	CP	AL	Bias	RMSE	CP	AL	Bias	RMSE	CP	AL	Bias	RMSE	CP	AL
LM	0.08	0.09	0.40	0.10	0.19	0.21	0.42	0.15	11.84	12.75	0.42	7.83	12.31	14.17	0.41	7.51
DPM	0.13	0.14	0.08	0.16	0.18	0.19	0.17	0.20	11.02	11.38	0.04	13.72	9.69	10.01	0.18	13.09
DDPM	0.09	0.09	0.29	0.14	0.19	0.20	0.06	0.19	10.41	10.84	0.09	13.50	9.79	10.10	0.07	11.83
EDDPM	0.02	0.03	0.97	0.15	0.06	0.08	0.80	0.20	-1.28	3.63	1.00	14.55	0.52	3.06	0.96	12.57

with  $3.0^2$  on the diagonal elements.

Table 2 presents the simulation results. Overall, the results consistently show that our methods have the smallest bias and RMSE across different scenarios, indicating EDDPM’s superior accuracy in point estimation. Turning to interval estimation, which is assessed by the coverage probability (CP) of 95% credible intervals, EDDPM stands out for its well-calibrated CP, closer to the target 95%. The linear model is sensitive to the latent treatment heterogeneity of the data-generating processes, yielding the worst performance across most metrics. Although the DPM and DDPM models improve upon the linear model, their performance falls short of the exemplary standards set by EDDPM. In practice, we recommend evaluating the performance of these models, as illustrated in Section 5.

## 5 An Illustrative Data Example

We demonstrate our proposed methods by analyzing the SPRINT dataset introduced in Section 1.1. Our primary goals include evaluating the causal estimands on recurrent hospital visits defined in Section 2.2, i.e., differences between the treatment and control groups in the expected number of hospital visits (SANR) and the average event rate (SAER) for always-survivors. Specifically, we consider  $\text{SANR}(t; r) = \mu^1(t; r)/\mu^0(t; r)$  and  $\text{SAER}(t; r) = \{\mu^1(t; r)/\tau^1(t; r)\}/\{\mu^0(t; r)/\tau^0(t; r)\}$ , for  $t < r$ . Understanding these aspects can clarify

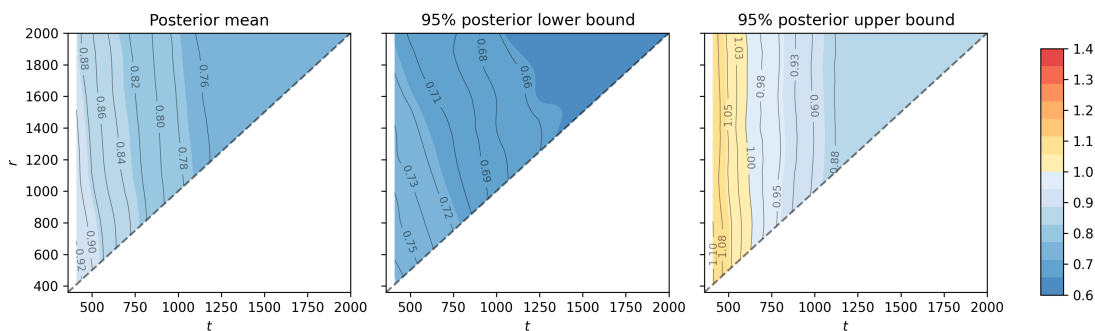


Figure 2: Contour plots of posterior mean (left), 95% posterior lower bound (middle), and upper bound (right) for SANR. The posterior values are computed for different cut-off values of  $t$  and  $r$  from 400 days ( $\approx 1$  year) to 2000 days ( $\approx 5$  years) with an increment of 200 such that  $t \leq r$ , and interpolated between the grid values with a cubic spline. The regions with the estimate greater than 1 are represented using warm colors (yellow to red), while regions with the estimate less than 1 are indicated using cool colors (blue).

whether and how structured exercise modifies not only the frequency but also the timing patterns of hospital visits, which are critical dimensions of clinical management and quality of life in patients with chronic heart failure. We perform inference using model (7) with proper, weakly informative conjugate priors for all parameters. Specifically, the chosen priors are identical to those used in the simulation study presented in Section 4. We set  $\rho = 0.5$  as the default correlation parameter and examine the sensitivity for different values.

We evaluate the predictive performance of the models using the log pseudo marginal likelihood (LPML; Geisser and Eddy, 1979). For the Bayesian models considered in simulations—LM, DPM, DDPM, and EDDPM—the LPML values are  $-21113.86$ ,  $-16397.04$ ,  $-15203.78$ , and  $-12245.87$ , respectively. Since a higher LPML indicates a better predictive fit in terms of LOO predictive densities, the EDDPM emerges as the superior model among the four models. We therefore focus on the EDDPM method in the subsequent discussion.

Figures 2 and 3 display contour plots of the posterior mean along with the corresponding 95% credible lower and upper surfaces, where the horizontal axis tracks follow-up time  $t$  and the vertical axis fixes the always-survivor subpopulation indexed by  $r$ . For SANR in Figure 2, the 95% upper surface remains almost entirely below 1.0 for  $t > 700$ , providing

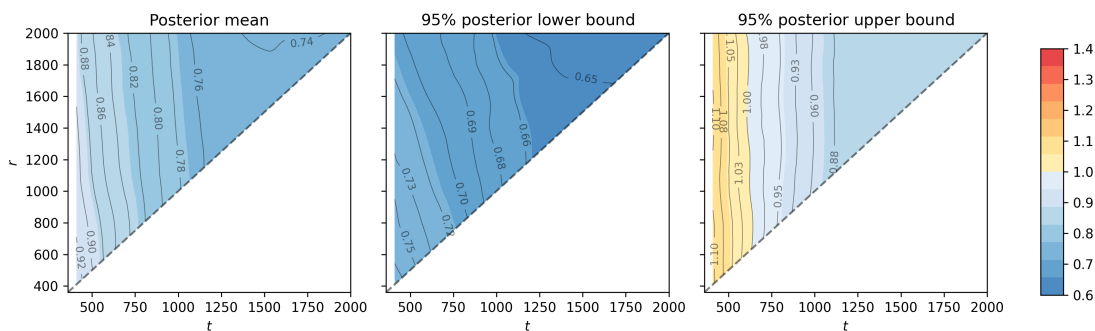


Figure 3: Contour plots of posterior mean (left), 95% posterior lower bound (middle), and upper bound (right) for SAER.

evidence that an intensive SBP reduces the expected number of recurrent major cardiovascular events over the long term; the posterior distributions also declines with increasing  $t$ , suggesting that the treatment effect becomes more pronounced as follow-up progresses. Similarly, the 95% upper surface of SAER in Figure 3 remains almost entirely below 1.0 for  $t > 700$ , showing evidence that the intensive SBP reduces the expected rate of recurrent major cardiovascular events over the long term. Across both estimands, treatment effects appear largely homogeneous with respect to  $r$ , indicating minimal effect-modification by this dimension.

To gauge the reliability of the Bayesian analyses for weakly identifiable models, we undertake a sensitivity analysis focusing on the unidentifiable frailty correlation parameter  $\rho$ . Specifically, we investigate how the posterior distribution of the SANR estimand responds to more extreme values of  $\rho \in \{0.1, 0.9\}$ , which represent weak and strong correlation between cross-world frailties, and hence potential outcomes. Figure 4 displays the resulting posterior estimates. Switching from  $\rho = 0.5$  to the lower correlation  $\rho = 0.1$  increases the upper bounds by roughly 0.01 – 0.1 across all time points, whereas switching to  $\rho = 0.9$  shift the posterior distributions only slightly. Importantly, even under these slight shifts, the upper bounds of the credible intervals decline with increasing  $t$  and remain below 1.0 for  $t > 1000$  for both extreme scenarios, indicating that the substantive conclusions are

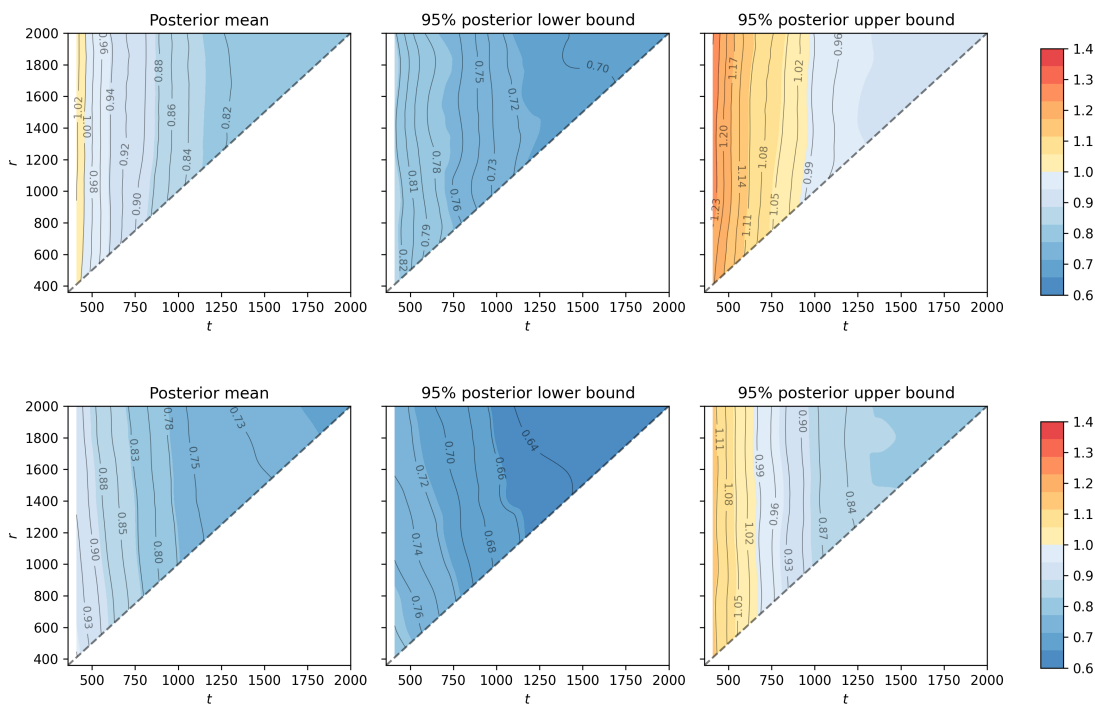


Figure 4: Posterior distributions of SANR under two alternative sensitivity parameters  $\rho$ , displayed vertically: top,  $\rho = 0.1$ ; bottom,  $\rho = 0.9$ .

unaffected, supporting the claim that intensive SBP control exerts a durable, clinically meaningful reduction in the expected number and rate of recurrent major cardiovascular events. Additional sensitivity analyses for additional values of  $\rho$  and for the SAER are provided in Web Appendix E.

## 6 Concluding Remarks

We proposed a new principal stratification approach for causal recurrent event analysis in the presence of semi-competing risks. Our first significant contribution is the introduction of new principal causal estimands. We critically examine the limitations inherent in the traditional definition of always-survivors within recurrent event analyses and propose a refined definition that more accurately reflects treatment effects on recurrent events over time. Our second methodological innovation is the adaptation of the EDDPM prior, which

incorporates a nested structure tailored for joint analyses of recurrent events with semi-competing risks and embeds covariate dependence into the prior. The EDDPM effectively captures distributional heterogeneity and the complex nested dependencies between recurrent and terminal events. Furthermore, it addresses and mitigates the unfavorable random partition structures induced by traditional DP priors, an issue commonly neglected in similar analyses. We provided a fully tractable Gibbs sampling algorithm for inference, along with a rigorous theoretical investigation into the random partition structure imposed by our proposed prior. Simulation studies demonstrate that our method significantly outperforms traditional DP-based methods in accuracy and robustness. The practical utility of our approach was further illustrated through an analysis of data from the SPRINT trial, a real-world randomized clinical trial.

We adopted a frailty approach to explicitly model the dependence between recurrent and terminal event processes. The frailty is modeled using our proposed nested EDP prior, which offers flexibility over restrictive parametric approaches (Nevo and Gorfine, 2022; Lyu et al., 2023) and resolves the undesirable random partitioning effects of existing works (e.g., Paulon et al., 2020). Alternatively, cross-world and within-world dependencies could also be modeled using copula-based methods, such as those proposed by Xu et al. (2022). Importantly, even within the copula framework, our nested prior remains potentially beneficial and applicable, offering advantages in terms of avoiding undesirable partition issues.

## Acknowledgement

Research in this article was supported by the United States National Institutes of Health (NIH), National Heart, Lung, and Blood Institute (NHLBI, grant number R01-HL168202). All statements in this report, including its findings and conclusions, are solely those of the

authors and do not necessarily represent the views of the NIH.

## References

- Antoniak, C. E. (1974). Mixtures of Dirichlet Processes with Applications to Bayesian Nonparametric Problems. *The Annals of Statistics* 2(6), 1152 – 1174.
- Burns, N. and M. J. Daniels (2023). Truncation approximation for enriched dirichlet process mixture models.
- Comment, L., F. Mealli, S. Haneuse, and C. Zigler (2019, 2). Survivor average causal effects for continuous time: a principal stratification approach to causal inference with semicompeting risks.
- Frangakis, C. E. and D. B. Rubin (2002). Principal stratification in causal inference. *Biometrics* 58, 21–29.
- Geisser, S. and W. F. Eddy (1979). A predictive approach to model selection. *Journal of the American Statistical Association* 74(365), 153–160.
- Lee, J., P. F. Thall, and S. H. Lin (2019). Bayesian semiparametric joint regression analysis of recurrent adverse events and survival in esophageal cancer patients. *The Annals of Applied Statistics* 13(1), 221 – 247.
- Li, F., P. Ding, and F. Mealli (2023). Bayesian causal inference: A critical review. *Philosophical Transactions of the Royal Society A: Mathematical, Physical and Engineering Sciences* 381(2247), 20220153.
- Lyu, T., B. Bornkamp, G. Mueller-Velten, and H. Schmidli (2023). Bayesian inference for a principal stratum estimand on recurrent events truncated by death. *Biometrics* 79(4), 3792–3802.
- Maceachern, S. (1999, 01). Dependent nonparametric processes. *Proceedings of the Section on Bayesian Statistical Science, American Statistical Association*, 50–55.
- Nevo, D. and M. Gorfine (2022, 10). Causal inference for semi-competing risks data. *Biostatistics* 23, 1115–1132.
- Paulon, G., M. D. Iorio, A. Guglielmi, and F. Ieva (2020, 1). Joint modeling of recurrent events and survival: A bayesian non-parametric approach. *Biostatistics* 21, 1–14.
- Robins, J. (1986). A new approach to causal inference in mortality studies with a sustained exposure period—application to control of the healthy worker survivor effect. *Mathematical Modelling* 7(9), 1393–1512.
- Rubin, D. B. (1978). Bayesian Inference for Causal Effects: The Role of Randomization. *The Annals of Statistics* 6(1), 34 – 58.

- SPRINT Research Group, J. T. Wright, Jr, J. D. Williamson, P. K. Whelton, J. K. Snyder, K. M. Sink, M. V. Rocco, D. M. Reboussin, M. Rahman, S. Oparil, C. E. Lewis, P. L. Kimmel, K. C. Johnson, D. C. Goff, Jr, L. J. Fine, J. A. Cutler, W. C.ushman, A. K. Cheung, and W. T. Ambrosius (2015, November). A randomized trial of intensive versus standard blood-pressure control. *N. Engl. J. Med.* *373*(22), 2103–2116.
- Stensrud, M. J., M. Valberg, K. Røysland, and O. O. Aalen (2017). Exploring selection bias by causal frailty models: The magnitude matters. *Epidemiology* *28*(3), pp. 379–386.
- Tian, X., M. Ciarleglio, J. Cai, E. J. Greene, D. Esserman, F. Li, and Y. Zhao (2024, 02). Bayesian semi-parametric inference for clustered recurrent events with zero inflation and a terminal event. *Journal of the Royal Statistical Society Series C: Applied Statistics* *73*(3), 598–620.
- van den Boom, W., M. D. Iorio, and M. Tallarita (2022). Bayesian inference on the number of recurrent events: A joint model of recurrence and survival. *Statistical Methods in Medical Research* *31*(1), 139–153. PMID: 34812661.
- Wade, S., S. Mongelluzzo, and S. Petrone (2011). An enriched conjugate prior for Bayesian nonparametric inference. *Bayesian Analysis* *6*(3), 359 – 385.
- Xu, Y., D. Scharfstein, P. Müller, and M. Daniels (2022, 1). A bayesian nonparametric approach for evaluating the causal effect of treatment in randomized trials with semi-competing risks. *Biostatistics* *23*, 34–49.
- Xu, Z., D. Sinha, and J. R. Bradley (2021, 2). Joint analysis of recurrence and termination: A bayesian latent class approach. *Statistical Methods in Medical Research* *30*, 508–522.
- Yu, T., M. Peng, Y. Cui, E. Chen, and C. Chen (2024). Exploring causal effects of hormone- and radio-treatments in an observational study of breast cancer using copula-based semi-competing risks models.
- Zehavi, T., U. Obolski, M. Chowers, and D. Nevo (2025). Causal effects on non-terminal event time with application to antibiotic usage and future resistance.
- Zhang, J. L. and D. B. Rubin (2003). Estimation of causal effects via principal stratification when some outcomes are truncated by “death”. *Journal of Educational and Behavioral Statistics* *28*(4), 353–368.

## A On event rate estimand

When rate ratio estimand is of interest, an alternative definition is the *equal-weighted* event rate among the always-survivors, given by  $\bar{\lambda}^1(t; r)/\bar{\lambda}^0(t; r)$ , with  $\bar{\lambda}^z(t; r) = \mathbb{E}[N_i^z(t)/T_{iN_i^z(t)} \mid \mathcal{AS}(r)]$ . In this definition, each always-survivor is weighted equally regardless of their follow-up exposure time. This distinction matters when death or withdrawal truncates observation: early deaths generate exceedingly small denominators, inflating the variance. In contrast, the  $\text{SAER}(t; r)$  estimand is constructed as the exposure-weighted rate ratio pooling total events and total exposure time before division. Mathematically, we can write

$$\frac{\mu^z(t; r)}{\tau^z(t; r)} = \mathbb{E} \left[ \omega_i(t; r) \times \frac{N_i^z(t)}{T_{iN_i^z(t)}} \mid \mathcal{AS}(r) \right], \quad \text{with} \quad \omega_i(t; r) = \frac{T_{iN_i^z(t)}^z}{\tau^z(t; r)}.$$

Hence it is evident that  $\text{SAER}(t; r)$  downweights units who are observed for only a short period, and dynamically adjusts for differential survival, providing a direct public health interpretation in terms of events prevented per person-time. These properties render the exposure-weighted formulation more interpretable and operationally convenient than its equal-weighted counterpart for causal recurrent-event analyses in the presence of a competing risk of death.

## B A potential pitfall of DP

### B.1 DP for the recurrent event analysis with a terminal event

As recent non-causal descriptive analyses for recurrent processes with a terminal event, Paulon et al. (2020) jointly modeled the gap times of recurrent and terminal events using a Dirichlet process mixture model with log-normal kernels for both the subject-specific frailty

parameter and the error term. Tian et al. (2024) used a DP prior for the scale parameter of Gumbel (extreme value distribution) error terms for the log-scaled survival time. These joint DP models of the log-transformed gap times and survival times, i.e.,  $Y_{ij}^z = \log(W_{ij}^z)$  and  $U_i^z = \log(D_i^z)$ , are typically specified as follows:

$$U_i, \bar{Y}_i | P \sim f(u, \bar{y} | P) = \int K(u, \bar{y} | \xi) dP(\xi) = \sum_{j=1}^{\infty} w_j K(u, \bar{y} | \xi_j), \quad (11)$$

where  $\bar{Y}_i = (Y_{i1}, \dots, Y_{iN_i})^\top$ ,  $U_i$  is univariate,  $K(\cdot)$  is an appropriate kernel function, and the mixing distribution  $P$  is given a DP prior with scale parameter  $\alpha > 0$  and base measure  $P_0$ , denoted by  $P \sim \text{DP}(\alpha, P_0)$ . The second equation follows from the a.s. discrete nature of the DP, that is, the model reduces to a countable mixture with the mixing weights  $w_j$  have a stick breaking prior with parameter  $\alpha$  and  $\xi_j \sim P_0$  independently of the  $w_j$ . This model can be alternatively described as the following hierarchical model:  $U_i | \theta_i \sim F_u(\cdot | \phi_i, \gamma_i)$ ,  $\bar{Y}_i | \theta_i \sim F_{\bar{y}}(\cdot | \theta_i, \gamma_i)$ ,  $(\phi_i, \theta_i, \gamma_i) | P \sim P$ ,  $P \sim \text{DP}(\alpha, P_{0\phi} \times P_{0\theta} \times P_{0\gamma})$ , where the atom  $\xi_i$  is decomposed into  $\phi_i$  and  $\theta_i$ , which are survival and recurrent parameters, respectively. Here the base measure  $P_{0\phi}$  and  $P_{0\theta}$  of the DP assumes independence between  $\phi$  and  $\theta$ . We further assume that  $P_{0\phi}$  and  $P_{0\theta}$  are absolutely continuous, admitting densities  $p_{0\phi}$  and  $p_{0\theta}$ . Then (11) can be written as  $f(u, \bar{y} | P) = \sum_{j=1}^{\infty} w_j K(u | \bar{y}, \phi_j) K(\bar{y} | \theta_j)$ , where  $K(u | \bar{y}, \phi)$  and  $K(\bar{y} | \theta)$  are the densities associated to  $F_u(\cdot | \bar{y}, \phi)$  and  $F_{\bar{y}}(\cdot | \theta)$ .

While this is a simple, common approach adopted in literature for the joint analysis of recurrent events with a terminal event (Lee et al., 2019; Paulon et al., 2020; Xu et al., 2021; van den Boom et al., 2022; Xu et al., 2022; Tian et al., 2024; Zehavi et al., 2025), a potential pitfall of these joint specifications is that the latent random partition induced by the DP will be overwhelmingly determined by the recurrent events rather than the terminal event as the number of recurrences grows. This issue occurs because the likelihood contribution

of the recurrent event dominates that of a single terminal event, which may not even be observed due to other censoring events. Consequently, the DP prior favors a random partition that approximates the distribution of the recurrent events well with as many clusters as necessary. However, having too many small clusters, which are dominantly determined by the contribution of  $\bar{y}$ , can lead to unreliable within-cluster predictions of the survival event  $u$ , with higher posterior variance due to unnecessarily small sample sizes, thereby compromising the predictive performance for the survival event. Predictive performance is crucial for Bayesian causal inference because the inferential procedure imputes missing potential outcomes and, therefore, heavily depends on the accuracy of potential outcome predictions. Additionally, existing approaches use the joint DP primarily to model a frailty term. However, because the frailty is widely recognized as a subject-specific distinct parameter that reflects an individual’s vulnerability (e.g., physical health conditions), it is somewhat counterintuitive that the random partition, which yields the subject-specific frailty, is driven largely by numerous recurrent events rather than the subject-specific survival event.

## B.2 Random partition induced by the standard DP

This section discusses the adverse impact of the standard DP random partition on predictive performance for recurrent outcomes with truncation by death. Let  $\mathcal{P}_n = (s_1, \dots, s_n)$  be the random partition defined by cluster allocation labels, where  $s_i = j$  if  $(\phi_i, \theta_i)$  equals the  $j$ -th unique value  $(\phi_j^*, \theta_j^*)$ , for  $j = 1, \dots, M_n$ . Here,  $M_n$  is the number of distinct groups (clusters) in the partition  $\mathcal{P}_n$ . For each cluster  $j$ , let  $\mathcal{S}_j = \{i : s_i = j\}$  be the set of indices for individuals assigned to the  $j$ -th cluster. Define  $\bar{Y}_j^* = \{\bar{Y}_i : i \in \mathcal{S}_j\}$ ,  $U_j^* = \{U_i : i \in \mathcal{S}_j\}$ , and let  $\bar{Y}_{1:n} = (\bar{Y}_1, \dots, \bar{Y}_n)$ ,  $U_{1:n} = (U_1, \dots, U_n)$ .

Under this setup, the joint posterior distribution of the random partition  $\mathcal{P}_n$  and the

cluster-specific parameters  $(\phi^*, \theta^*) = (\phi_j^*, \theta_j^*)_{j=1}^{M_n}$  is given by

$$p(\mathcal{P}_n, \phi^*, \theta^* | \bar{Y}_{1:n}, U_{1:n}) \propto p(\mathcal{P}_n) \prod_{j=1}^{M_n} p_{0\phi}(\phi_j^*) p_{0\theta}(\theta_j^*) \prod_{j=1}^{M_n} \prod_{i \in \mathcal{S}_j} K(U_i | \bar{Y}_i, \phi_j^*) K(\bar{Y}_i | \theta_j^*). \quad (12)$$

The prior on the random partition induced by the DP is  $p(\mathcal{P}_n) \propto \alpha^{M_n} \prod_{j=1}^{M_n} \Gamma(n_j)$ , where  $n_j = |\mathcal{S}_j|$  (Antoniak, 1974) and  $\alpha$  is a precision parameter of the DP. Consequently, the posterior distribution of the random partition  $\mathcal{P}_n$  can be written as

$$p(\mathcal{P}_n | \bar{Y}_{1:n}, U_{1:n}) \propto \alpha^{M_n} \prod_{j=1}^{M_n} \Gamma(n_j) h_u(U_j^* | \bar{Y}_j^*) h_y(\bar{Y}_j^*), \quad (13)$$

where  $h_u(U_j^* | \bar{Y}_j^*) = \int_{\Phi} \prod_{i \in \mathcal{S}_j} K(U_i | \bar{Y}_i, \phi) dP_{0\phi}(\phi)$  and  $h_y(\bar{Y}_j^*) = \int_{\Theta} \prod_{i \in \mathcal{S}_j} K(\bar{Y}_i | \theta) dP_{0\theta}(\theta)$ .

From (12), the posterior distributions of the cluster-specific parameters are

$$p(\phi_j^* | \mathcal{P}_n, \bar{Y}_{1:n}, U_{1:n}) \propto p_{0\phi}(\phi_j^*) \prod_{i \in \mathcal{S}_j} K(U_i | \bar{Y}_i, \phi_j^*), \quad (14)$$

$$p(\theta_j^* | \mathcal{P}_n, \bar{Y}_{1:n}, U_{1:n}) \propto p_{0\theta}(\theta_j^*) \prod_{i \in \mathcal{S}_j} K(\bar{Y}_i | \theta_j^*).$$

(13) indicates that, under the DP partition, individuals are grouped according to similarities in recurrent outcomes and their relationship to the survival outcome. When multiple recurrences are observed, the likelihood term involving  $\bar{Y}$  often dominates the posterior in (13). However, from (14), the posteriors of each cluster's parameters  $\phi_j^*$  and  $\theta_j^*$  are updated by observations of all individuals in the shared subset  $\mathcal{S}_j$ . Consequently, the posterior of  $\phi_j^*$  may fail to capture local trends of survival events if the partition is driven largely by the recurrent events. Moreover, if many clusters are needed to approximate the distribution of recurrent outcomes (i.e., if  $M_n$  is large), each cluster may contain relatively few observations. In that case, the posterior for  $\phi_j^*$  is inferred from an unnecessarily small

sample, yielding an unreliable mean estimate and large posterior variance, with the prior continuing to exert strong influence.

## C Proofs

### C.1 Proof of Proposition 1

*Proof.* Independence of conditional distributions on  $\phi \in \Phi$  implies that

$$p(\mathcal{P}_n, \phi^*) = p(\mathcal{P}_{n,u}) \prod_{j=1}^{M_n} p_{0\phi}(\phi_j^*) p(\mathcal{P}_{n,y} | \mathcal{P}_{n,u}, \phi_j^*) = p(\mathcal{P}_{n,u}) \prod_{j=1}^{M_n} p_{0\phi}(\phi_j^*) p(\mathcal{P}_{n,y} | \phi_j^*) \quad (15)$$

The result of Antoniak (1974) implies that the random partition induced by the DP is

$$p(\mathcal{P}_{n,u}) = \frac{\Gamma(\alpha_\phi)}{\Gamma(\alpha_\phi+n)} \alpha_\phi^{M_n} \prod_{j=1}^{M_n} \Gamma(n_j) \quad \text{and} \quad p(\mathcal{P}_{n,y} | \phi_j^*) = \frac{\Gamma(\alpha_\theta(\phi_j^*))}{\Gamma(\alpha_\theta(\phi_j^*)+n_j)} \alpha_\theta(\phi_j^*)^{M_{n,j}} \prod_{l=1}^{M_{n,j}} \Gamma(n_{lj}).$$

Putting these into (15) and integrating out  $\phi^*$ , we obtain the desired result for the first part of the proposition. The second part of the proposition can be obtained by the Bayes theorem.  $\square$

### C.2 Proof of Theorem 1

*Proof.* We consider the identification of (1). For any  $r \in (t, C^*]$ , we have

$$\begin{aligned} \Pr(N_i^z(t) = n | \mathcal{AS}(r)) &= \Pr\left(N_i^z(t) = n \mid T_{iN_i^1(r)}^1 < D_i^1, T_{iN_i^0(r)}^0 < D_i^0\right) \\ &= \mathbb{E}_{X,\gamma|\mathcal{AS}(r)} \left[ \Pr\left(N_i^z(t) = n \mid T_{iN_i^1(r)}^1 < D_i^1, T_{iN_i^0(r)}^0 < D_i^0, X, \gamma\right) \right] \\ &= E_{X,\gamma|\mathcal{AS}(r)} \left[ \frac{\Pr\left(N_i^z(t) = n, T_{iN_i^1(r)}^1 < D_i^1, T_{iN_i^0(r)}^0 < D_i^0 \mid X, \gamma\right)}{\Pr\left(T_{iN_i^1(r)}^1 < D_i^1, T_{iN_i^0(r)}^0 < D_i^0 \mid X, \gamma\right)} \right] \\ &= E_{X,\gamma|\mathcal{AS}(r)} \left[ \frac{\Pr\left(N_i^z(t) = n, T_{iN_i^z(r)}^z < D_i^z \mid X, \gamma\right) \Pr\left(T_{iN_i^{1-z}(r)}^z < D_i^{1-z} \mid X, \gamma\right)}{\Pr\left(T_{iN_i^1(r)}^1 < D_i^1 \mid X, \gamma\right) \Pr\left(T_{iN_i^0(r)}^0 < D_i^0 \mid X, \gamma\right)} \right] \end{aligned}$$

$$\begin{aligned}
&= E_{X,\gamma|\mathcal{AS}(r)} \left[ \Pr \left( N_i^z(t) = n \mid T_{iN_i^z(r)}^z < D_i^z, X, \gamma \right) \right] \\
&= E_{X,\gamma|\mathcal{AS}(r)} \left[ \Pr \left( N_i^z(t) = n \mid Z_i = z, T_{iN_i^z(r)}^z < D_i^z, X, \gamma \right) \right] \\
&= E_{X,\gamma|\mathcal{AS}(r)} \left[ \Pr \left( N_i(t) = n \mid Z_i = z, T_{iN_i(r)} < D_i, X, \gamma \right) \right] \\
&= \int_{\mathcal{X}} \int_0^\infty \Pr \left( N_i(t) = n \mid Z_i = z, T_{iN_i(r)} < D_i, X, \gamma \right) f_{X,\gamma|\mathcal{AS}(r)}(x, \gamma) d\gamma dx.
\end{aligned}$$

The second line is by the law of iterated expectations, the fourth line is by Assumption 4, the sixth line is by Assumption 2, and the seventh line is by Assumption 1. Now note that

$$\begin{aligned}
f_{X,\gamma|\mathcal{AS}(r)}(x, \gamma) &= \frac{\Pr \left( T_{iN_i^1(r)}^1 < D_i^1, T_{iN_i^0(r)}^0 < D_i^0 \mid \mathbf{X}_i = \mathbf{x}, \gamma \right) f_\gamma(\gamma) f_X(x)}{\int_{\mathcal{X}} \int_0^\infty \Pr \left( T_{iN_i^1(r)}^1 < D_i^1, T_{iN_i^0(r)}^0 < D_i^0 \mid \mathbf{X}_i = \mathbf{x}', \gamma' \right) f_\gamma(\gamma') f_X(x') d\gamma' dx'} \\
&= \frac{\Pr \left( T_{iN_i^1(r)}^1 < D_i^1 \mid \mathbf{X}_i = \mathbf{x}, \gamma \right) \Pr \left( T_{iN_i^0(r)}^0 < D_i^0 \mid \mathbf{X}_i = \mathbf{x}, \gamma \right) f_\gamma(\gamma) f_X(x)}{\int_{\mathcal{X}} \int_0^\infty \Pr \left( T_{iN_i^1(r)}^1 < D_i^1 \mid \mathbf{X}_i = \mathbf{x}', \gamma' \right) \Pr \left( T_{iN_i^0(r)}^0 < D_i^0 \mid \mathbf{X}_i = \mathbf{x}', \gamma' \right) f_\gamma(\gamma') f_X(x') d\gamma' dx'} \\
&= \frac{\Pr \left( T_{iN_i^1(r)}^1 < D_i^1 \mid Z_i = 1, \mathbf{X}_i = \mathbf{x}, \gamma \right) \Pr \left( T_{iN_i^0(r)}^0 < D_i^0 \mid Z_i = 0, \mathbf{X}_i = \mathbf{x}, \gamma \right) f_\gamma(\gamma) f_X(x)}{\int_{\mathcal{X}} \int_0^\infty \Pr \left( T_{iN_i^1(r)}^1 < D_i^1 \mid Z_i = 1, \mathbf{X}_i = \mathbf{x}', \gamma' \right) \Pr \left( T_{iN_i^0(r)}^0 < D_i^0 \mid Z_i = 0, \mathbf{X}_i = \mathbf{x}', \gamma' \right) f_\gamma(\gamma') f_X(x') d\gamma' dx'} \\
&= \frac{\Pr \left( T_{iN_i(r)} < D_i \mid Z_i = 1, \mathbf{X}_i = \mathbf{x}, \gamma \right) \Pr \left( T_{iN_i(r)} < D_i \mid Z_i = 0, \mathbf{X}_i = \mathbf{x}, \gamma \right) f_\gamma(\gamma) f_X(x)}{\int_{\mathcal{X}} \int_0^\infty \Pr \left( T_{iN_i(r)} < D_i \mid Z_i = 1, \mathbf{X}_i = \mathbf{x}', \gamma' \right) \Pr \left( T_{iN_i(r)} < D_i \mid Z_i = 0, \mathbf{X}_i = \mathbf{x}', \gamma' \right) f_\gamma(\gamma') f_X(x') d\gamma' dx'} \\
&= \frac{\eta_r(1, x, \gamma) \eta_r(0, x, \gamma) f_\gamma(\gamma) f_X(x)}{\int_{\mathcal{X}} \int_0^\infty \eta_r(1, x, \gamma) \eta_r(0, x, \gamma) f_\gamma(\gamma') f_X(x') d\gamma' dx'},
\end{aligned}$$

where the first line follows from Bayes' theorem, the second line follows from Assumption 4, the third line follows from Assumption 2, and the fourth line follows from Assumption 1. It is easy to show that (2) can be identified in the same manner.  $\square$

## D Details of Gibbs sampler

The posterior distributions of the parameters are obtained from the Markov chain Monte Carlo method. We develop a fully tractable Gibbs sampler that uses the data augmentation

method to impute truncated survival and gap times for each unit at both treatment arms and the cluster memberships induced by the EDDP, and exploit the complete likelihood to update the parameters. Specifically, we iterate between drawing from the conditional distributions of model parameters, potential outcomes, and latent nested cluster memberships given the other variables, respectively. The essential algorithm proceeds as follows:

1. Given all model parameters,  $G_i$  and  $H_i$ , sample  $Y_{i(N_i+1)}^*$  and  $U_i^*$ .
2. Given all model parameters,  $Y_{i(N_i+1)}^*$  and  $U_i^*$ , sample  $G_i$  and  $H_i$ .
3. Given  $Y_{i(N_i+1)}^*$ ,  $U_i^*$ ,  $G_i$  and  $H_i$ , sample all model parameters.
4. Compute the estimands.

For simplicity, in what follows, we denote by  $\mathbf{X}_i$  the augmented covariates that contain the baseline covariates and treatment variable  $Z_i$  and denote by  $\mathbf{X}_{ij}$  the covariates that additionally include the time-varying covariates at the  $j$ -th recurrent period  $\mathbf{V}_{ij}$ .

## D.1 Imputation of $U$

For each subject  $i$  with  $\delta_i^C = 1$ , given  $G_i$ ,  $\boldsymbol{\gamma} = (\gamma_1^{Z_i}, \dots, \gamma_K^{Z_i})$ ,  $\boldsymbol{\beta}_u = (\beta_{u,1}, \dots, \beta_{u,K})$ ,  $\boldsymbol{\tau}^2 = (\tau_1^2, \dots, \tau_K^2)$  and observed variables, we sample

$$U_i \mid - \sim \text{TN}(\mathbf{X}_i^\top \boldsymbol{\beta}_{u,G_i} + \gamma_{G_i}^{Z_i}, \tau_{G_i}^2, U_i^{\text{obs}}, \infty),$$

where  $\text{TN}(\mu, \sigma^2, l, u)$  denotes the truncated normal distribution with the mean, variance, lower bound, and upper bound parameters. If  $\delta_i^C = 0$  (death),  $U_i$  remains unchanged.

## D.2 Imputation of $Y_{i(N_i+1)}$

For each subject  $i = 1, \dots, n$ , given  $G_i, H_i, \boldsymbol{\gamma}, \boldsymbol{\beta}_y = ((\beta_{y,1|1}, \dots, \beta_{y,1|K})^\top, \dots, (\beta_{y,L|1}, \dots, \beta_{y,L|K})^\top)$ ,  $\boldsymbol{\sigma}^2 = ((\sigma_{1|1}^2, \dots, \sigma_{1|K}^2)^\top, \dots, (\sigma_{L|1}^2, \dots, \sigma_{L|K}^2)^\top)$ ,  $\boldsymbol{\psi} = ((\psi_{1|1}, \dots, \psi_{1|K})^\top, \dots, (\psi_{L|1}, \dots, \psi_{L|K})^\top)$ , and observed variables, we sample

$$Y_{i(N_i+1)} | - \sim \text{TN}(\mathbf{X}_{i(N_i+1)}^\top \boldsymbol{\beta}_{y, H_i | G_i} + \psi_{H_i | G_i} \gamma_{G_i}^{Z_i}, \sigma_{H_i | G_i}^2, Y_{i(N_i+1)}^{\text{obs}}, \infty),$$

where  $Y_{i(N_i+1)}^{\text{obs}} = \log(\mathcal{T}_i - T_{iN_i})$ .

## D.3 Update of G and H

For each  $i$ , given all parameters and observed/imputed  $U_i$  and  $Y_{ij}$ ,

$$p(G_i = k | -) \propto w_k^\phi \times \underbrace{\text{N}(U_i | \mathbf{X}_i \boldsymbol{\beta}_{u,k} + \gamma_k^{Z_i}, \tau_k^2)}_{\text{survival part}} \times \underbrace{\prod_{j=1}^{N_i+1} \sum_{l=1}^L [w_{l|k}^\theta \text{N}(Y_{ij} | \mathbf{X}_{ij} \boldsymbol{\beta}_{y,l|k} + \psi_{l|k} \gamma_k^{Z_i}, \sigma_{l|k}^2)]}_{\text{recurrent part}}.$$

Normalize over  $k = 1, \dots, K$  to obtain a categorical distribution and sample  $G_i$ . Then, for each  $i$  and  $j$ , we sample

$$p(H_{ij} = l | -) \propto w_{l|G_i}^\theta \times \phi\left(Y_{ij} \mid \mathbf{X}_{ij} \boldsymbol{\beta}_{y,l|G_i} + \psi_{l|G_i} \gamma_{G_i}^{Z_i}, \sigma_{l|G_i}^2\right),$$

and then sample  $H_{ij}$  from this  $l = 1, \dots, L$  categorical distribution.

#### D.4 Update of $w_k^\phi$ and $v_k^\phi$

Let  $v_K^\phi = 1$ . Given  $\alpha_\phi$  and  $G_i$ , draw  $v_k^\phi$  for  $k = 1, \dots, K - 1$  from

$$v_k^\phi \sim \text{Be} \left( 1 + \sum_{i=1}^n \mathbb{1}(G_i = k), \alpha + \sum_{i=1}^n \mathbb{1}(G_i > k) \right). \quad (16)$$

Then update  $w_k^\phi = v_k^\phi \prod_{j=1}^{k-1} (1 - v_j^\phi)$ .

#### D.5 Update of $w_{l|k}^\theta$ and $v_{l|k}^\theta$

For each class  $k$ , let  $v_{L|k}^\theta = 1$ . Given  $\alpha_{\theta|k}$  and  $H_{ij}$ , draw  $v_{l|k}^\theta$  for  $l = 1, \dots, L - 1$  from

$$v_{l|k}^\theta \sim \text{Be} \left( 1 + \sum_{i=1}^n \sum_{j=1}^{N_i} \mathbb{1}(H_{ij} = l, G_i = k), \alpha_{\theta|k} + \sum_{i=1}^n \sum_{j=1}^{N_i} \mathbb{1}(H_{ij} > l, G_i = k) \right). \quad (17)$$

Then update  $w_{l|k}^\theta = v_{l|k}^\theta \prod_{j=1}^{l-1} (1 - v_{j|k}^\theta)$  for  $k = 1, \dots, K$ .

#### D.6 Update of $\alpha_\phi$ and $\alpha_{\theta|k}$

Assuming a common conjugate prior  $\alpha_\phi, \alpha_{\theta|k} \sim \text{Ga}(a_\alpha, b_\alpha)$ , update the concentration parameters  $\alpha_\phi$  and  $\alpha_{\theta|k}$  for  $k = 1, \dots, K$ :

$$\begin{aligned} \alpha_\phi &\sim \text{Ga} \left( a_\alpha + K - 1, b_\alpha - \sum_{k=1}^{K-1} \ln(1 - w_k^\phi) \right), \\ \alpha_{\theta|k} &\sim \text{Ga} \left( a_\alpha + L - 1, b_\alpha - \sum_{l=1}^{L-1} \ln(1 - w_{l|k}^\theta) \right). \end{aligned}$$

## D.7 Update of $(\beta_{u,k}, \tau_k)$

For each upper-level component  $k$ , let  $n_k$  be the number of subjects  $i$  with  $G_i = k$ . Denote  $U_k$  and  $\mathbf{X}_k$  the stacked  $U_i$  and covariates for those subjects. We have:

$$\begin{aligned} \tau_k^2 \mid - &\sim \text{IG} \left( a_\tau + \frac{n_k}{2}, b_\tau + \frac{1}{2} \sum_{i:G_i=k} (U_i - \mathbf{X}_i \beta_{u,k} - \gamma_k^{Z_i})^2 \right), \\ \beta_{u,k} \mid - &\sim \text{MVN}(\Sigma_k \mathbf{X}_k^\top (U_k - \boldsymbol{\gamma}_{n_k}), \tau_k^2 \Sigma_k), \quad \Sigma_k = (\mathbf{X}_k^\top \mathbf{X}_k + \tau_k^2 \Sigma_{\beta_u}^{-1})^{-1}, \end{aligned}$$

where  $\boldsymbol{\gamma}_{n_k} = (\gamma_k^{Z_{k_1}}, \dots, \gamma_k^{Z_{k_{n_k}}})^\top$  is a column vector of size  $n_k$  and  $k_1, \dots, k_{n_k}$  are index of subjects with  $G_i = k$ .

## D.8 Update of $(\beta_{y,l|k}, \sigma_{l|k})$

Similarly, for the recurrent part, each pair  $(l \mid k)$  uses data from events where  $G_i = k$  and  $H_{ij} = l$ . Let  $n_{l|k}$  be that count,  $Y_{l|k}$  the stacked responses, and  $\mathbf{X}_{l|k}$  the corresponding covariates. Then

$$\begin{aligned} \sigma_{l|k}^2 \mid - &\sim \text{IG} \left( a_\sigma + \frac{n_{l|k}}{2}, b_\sigma + \frac{1}{2} \sum_{i,j:G_i=k, H_{ij}=l} (Y_{ij} - \mathbf{X}_{ij} \beta_{y,l|k} - \psi_{l|k} \gamma_k^{Z_i})^2 \right), \\ \beta_{y,l|k} \mid - &\sim \text{MVN}(\Sigma_{l|k} \mathbf{X}_{l|k}^\top (Y_{l|k} - \psi_{l|k} \boldsymbol{\gamma}_{n_{l|k}}), \sigma_{l|k}^2 \Sigma_{l|k}), \quad \Sigma_{l|k} = (\mathbf{X}_{l|k}^\top \mathbf{X}_{l|k} + \sigma_{l|k}^2 \Sigma_{\beta_y}^{-1})^{-1}. \end{aligned}$$

where  $\boldsymbol{\gamma}_{n_{l|k}} = (\gamma_k^{Z_{k_1}}, \dots, \gamma_k^{Z_{k_{n_{l|k}}}})^\top$  is a column vector of size  $n_{l|k}$  and  $k_1, \dots, k_{n_{l|k}}$  are index of subjects with  $G_i = k$  and  $H_{ij} = l$ .

## D.9 Update of $\gamma_k$

We update  $\gamma_k^0$  and  $\gamma_k^1$  one by one. For the frailty parameter, for each  $k$ :

$$\gamma_k^z \mid - \sim \text{N}(\mu_k, s_k),$$

where

$$\begin{aligned} s_k^{-1} &= \frac{1}{(1-\rho^2)\sigma_{\gamma_z}^2} + \frac{n_k^z}{\tau_k^2} + \sum_{l=1}^L \frac{n_{l|k}^z \psi_{l|k}^2}{\sigma_{l|k}^2}, \\ \mu_k &= s_k \left( \frac{\mu_{\gamma_z}}{(1-\rho^2)\sigma_{\gamma_z}^2} + \frac{\rho(\gamma_k^{1-z} - \mu_{\gamma_{1-z}})}{(1-\rho^2)\sigma_{\gamma_z}\sigma_{\gamma_{1-z}}} + \frac{1}{\tau_k^2} \sum_{i:Z_i=z,G_i=k} (U_i - \mathbf{X}_i\beta_{u,k}) \right. \\ &\quad \left. + \sum_{l=1}^L \frac{\psi_{l|k}}{\sigma_{l|k}^2} \sum_{i,j:Z_i=z,G_i=k,H_{ij}=l} (Y_{ij} - \mathbf{X}_{ij}\beta_{y,l|k}) \right), \end{aligned}$$

where  $n_k^z$  be the count of units with  $Z_i = z$  and  $G_i = k$ , and  $n_{l|k}^z$  be the count of units with  $Z_i = z$ ,  $G_i = k$  and  $H_{ij} = l$ .

## D.10 Update of $\psi_{l|k}$

Finally, the modulation term  $\psi_{l|k}$  capturing how  $\gamma_k^{Z_i}$  contributes the recurrent-event likelihood is updated by:

$$\psi_{l|k} \mid - \sim \text{N}(\mu_{l|k}, s_{l|k}),$$

where

$$s_{l|k}^{-1} = \frac{1}{\sigma_{\psi}^2} + \frac{\sum_{i,j \in G_i=k, H_{ij}=l} (\gamma_k^{Z_i})^2}{\sigma_{l|k}^2}, \quad \mu_{l|k} = s_{l|k} \left( \frac{\mu_{\psi}}{\sigma_{\psi}^2} + \sum_{i,j \in G_i=k, H_{ij}=l} \frac{\gamma_k^{Z_i} (Y_{ij} - \mathbf{X}_{ij}\beta_{y,l|k})}{\sigma_{l|k}^2} \right).$$

## D.11 Compute estimands

Given all model parameters, we compute  $\kappa_{t,r}(z, x, \boldsymbol{\gamma})$ ,  $\zeta_{t,r}(z, x, \boldsymbol{\gamma})$  and  $\eta_r(z, x, \boldsymbol{\gamma})$ . They are not easy to compute in closed form due to the nonparametric nature of the proposed prior. Therefore we approximate them by the Monte carlo simulation within each MCMC iteration. For example, we approximate  $\kappa_{t,r}(z, x, \boldsymbol{\gamma}) \approx 1/R \sum_{r=1}^R N_i(t)$  with  $R$  simulated samples of  $N_i(t)$  from its posterior predictive distribution.

## E Sensitivity analysis

This section complements the empirical results in Section 5 with additional sensitivity analyses for the unidentifiable frailty parameter. Figures 5 and 6 report posterior surfaces for SANR and SAER obtained under five sensitivity parameters  $\rho \in \{0.1, 0.3, 0.5, 0.7, 0.9\}$ . Overall, varying the sensitivity parameters does not cause substantial shifts in the posterior estimates, so our substantive conclusions remain unchanged.

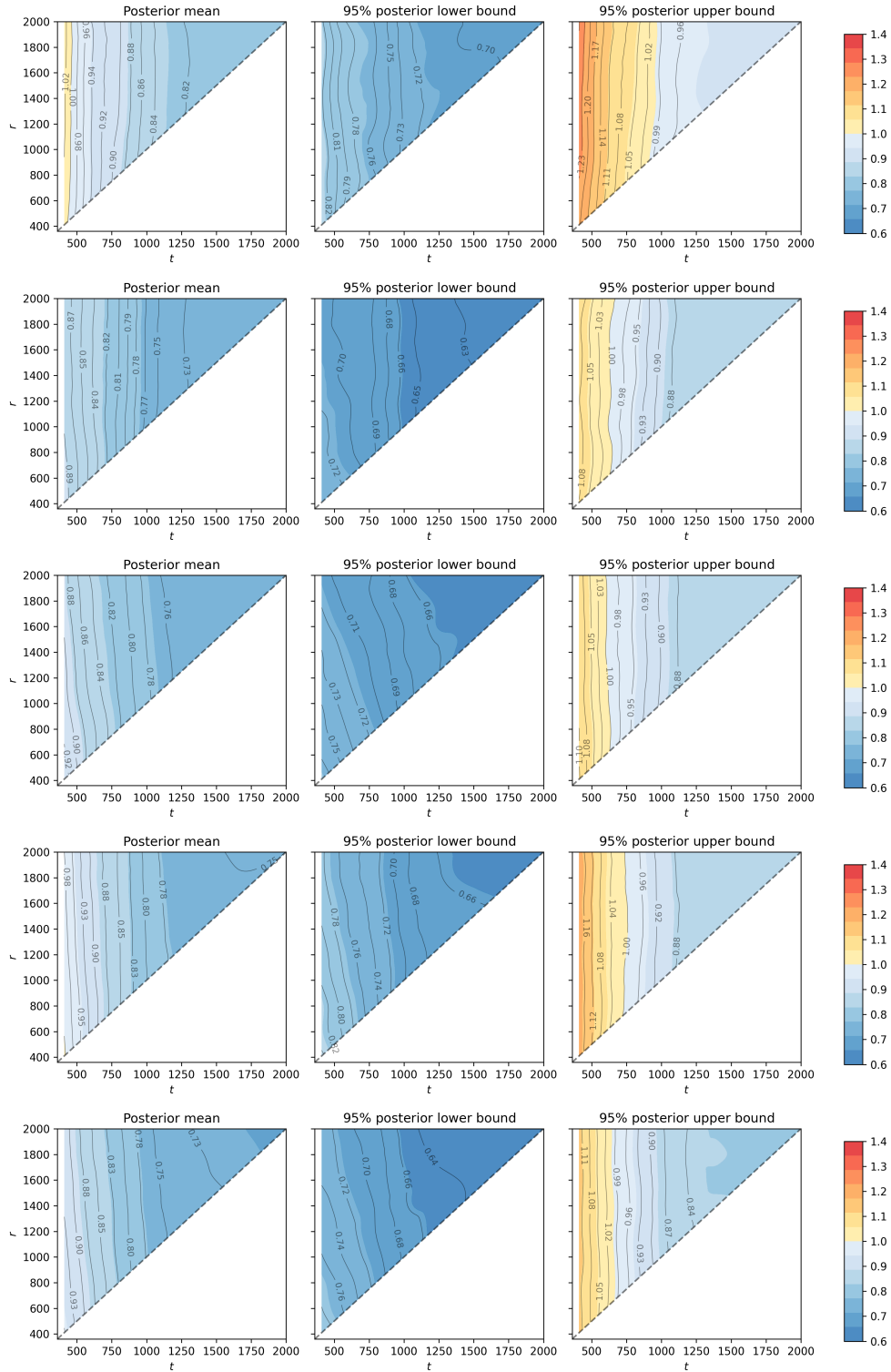


Figure 5: Posterior distributions of SANR under five sensitivity parameters ( $\rho = 0.1, 0.3, 0.5, 0.7, 0.9$ ), shown from top to bottom.

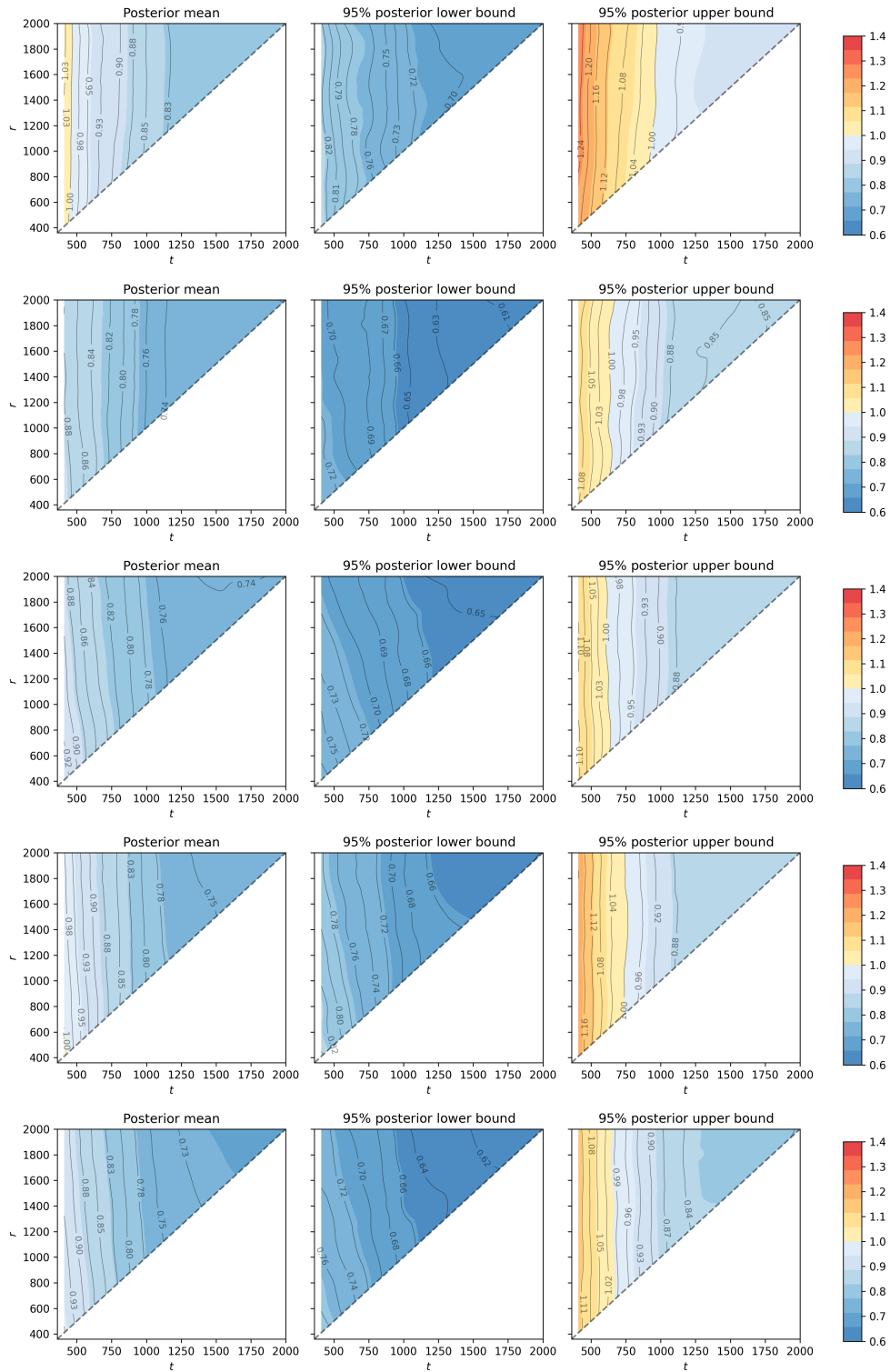


Figure 6: Posterior distributions of SAER under five sensitivity parameters ( $\rho = 0.1, 0.3, 0.5, 0.7, 0.9$ ), shown from top to bottom.